Charles University in Prague, Faculty of Science
Department of Cell Biology

Study program: Biology
Cell and Developmental Biology

Radek Jankele

Analysis of short Argonaute isoforms from mouse oocytes

Analýza krátkých isoforem proteinů Argonaut z myších oocytů

Diploma thesis / Diplomová práce

Supervisor: Doc. Petr Svoboda, Ph.D.

Institute of Molecular Genetics of the ASCR
Laboratory of Epigenetic Regulations
Prague 2015

Prohlášení:

Prohlašuji, že jsem tuto diplomovou práci zpracoval samostatně na základě konzultací se školitelem a že jsem uvedl všechny použité informační zdroje a literaturu. Tato práce ani její podstatná část nebyla předložena k získání jiného nebo stejného akademického titulu.

V Praze, 4. 5. 2015 Radek Jankele

Poděkování:

Na tomto místě chci v první řadě poděkovat mému školiteli Petru Svobodovi za nezištnou a nekončící podporu na startu mojí vědecké dráhy, výjimečné příležitosti, které mi zprostředkoval, za pomoc s touto prací, a za schovívavost k mojí pracovní morálce a dochvilnosti. Petr měl naprosto zásadní význam pro můj osobní rozvoj a na mojí budoucnost. Děkuji!

Bez neutuchající podpory mých milujících rodičů bych se jen stěží dopracoval až do závěru magisterského studia, kdy píšu tyto řádky. Nejen že mě přivedli na svět, ale vždy podporovali mého zvídavého ducha a nikdy neodbyli moje věčné otázky po smyslu všeho kolem nás, byť sami často neznali odpověď. Hodnoty, ke kterým mě vychovali, budu, pevně věřím, ctít po zbytek svého života. Děkuji, Mami a Tati!

Velký dík patří mým přátelům, zejména Janě Uhlířové, na kterou se mohu vždy spolehnout a jejíž věčný smích mě dokáže rozveselit za každých okolností. Nebýt Jany, umřel bych při psaní této práce hlady a trudomyslností. Za úžasnou dálkovou podporu a přilévání optimismu do žil vděčím mojí milé přítelkyni Lucii Kešnerové.

Obrovskou zásluhu (nejen) na této práci mají moji skvělí kolegové (přesněji řečeno, kolegyně) a kamarádky z naší laboratoře, díky kterým jsem se do práce vždycky těšil. Přál bych si tak skvělou atmosféru mít v týmu i v budoucnu. Nasadili jste laťku hodně vysoko a díky za to. Za obětavou pomoc a cenné rady mnohokrát děkuji zejména Radkovi Malíkovi a Janě Urbanové. Všem ostatním patří uznání za toleranci k mému chaosu a občasným nevysvětlitelným nehodám.

Abstrakt:

Proteiny z rodiny Argonautů, řízené malými molekulami RNA, představují konzervované jádro mechanismů umlčování RNA (RNA silencing). Tyto mechanismy potlačují produkci virů, šíření mobilní DNA, a regulují genovou expresi na základě sekvenční informace nesené asociovanou RNA. V somatických buňkách savců je dominantním mechanismem regulační microRNA (miRNA) dráha. Malé miRNA ovlivňují expresi většiny savčích genů. Argonaute proteiny inhibují translaci a indukují deadenylaci mRNA s částečnou homologií k navázané miRNA. Deadenylace obvykle vyústí degradaci mRNA. Těmito mechanismy miRNA dráha citlivě kontroluje hladiny produkovaných proteinů. Na rozdíl od příbuzného mechanismu RNA interference (RNAi) využívajícího katalyticky aktivní proteiny Argonaute schopné rozštěpit komplementárních molekuly RNA, miRNA umlčování je závislé na celé řadě dalších faktorů. Role miRNA regulace v komplexních biologických procesech od organogeneze, přes krvetvorbu až po rakovinu je dobře doložená. Myší oocyty postrádající kanonické miRNA jsou překvapivě schopné oplození a úspěšně projdou preimplantačním vývojem. Ani nejčetnější oocytární miRNA však nejsou sto efektivně umlčet cílové geny, přestože příbuzný mechanismus RNAi, sdílející s miRNA mechanismem klíčové enzymy, je v oocytech a časných embryích vysoce aktivní. Příčina snížené aktivity miRNA v myších vajíčkách je doposud neobjasněná. Tato diplomová práce pojednává o krátkých isoformách Argonautu, které byly objeveny v transkriptomu myších vajíček. Tyto jsou oproti Během mého výzkumu jsem vyizoloval mRNA kódující tyto krátké isoformy z myších oocytů a analyzoval jejich vliv na funkci miRNA a RNAi mechanismů v buněčných kulturách. S využitím luciferázového reporterového systému jsem zjistil, že ektopicky exprimované isoformy Argonautu neovlivňují aktivitu miRNA, ani RNAi v myších a lidských buňkách, a tedy pravděpodobně nefungují jako dominantně negativní inhibitor RNA umlčování.

Klíčová slova:

AGO, Argonaute, RNA, umlčování, siRNA, miRNA, interference, oocyt, RISC

Abstract:

Argonaute proteins carrying small RNAs form the conserved core of RNA silencing mechanisms, which repress viruses, mobile genetic elements, and genes in a sequence specific manner. The microRNA (miRNA) pathway is a dominant mammalian RNA silencing mechanism in somatic cells, which post-transcriptionally regulates large fraction of genes and thereby adjusts protein levels. miRNA-guided Argonautes inhibit translation and induce deadenylation of complementary mRNAs, ultimately resulting in their decay. In contrast to RNA interference (RNAi), which employs Argonaute slicer activity to directly cleave perfectly complementary RNAs, an effective miRNA-mediated mRNA repression requires multiple Argonaute-associated protein factors and enzymes. The miRNA pathway has been implicated in many complex biological processes ranging from organogenesis, stress-response to haematopoiesis or cancer. Surprisingly, canonical miRNAs are not essential for oocytes and early embryonic development in mice. Even the most abundant miRNAs present in mouse oocytes are unable to effectively repress target genes. However, RNAi, which shares key enzymes with the miRNA pathway, is highly active in oocytes and early embryos. The cause of miRNA inactivity in mouse oocytes remains unknown. This thesis is focused on short Argonaute isoforms encompassing Argonaute's N-terminal domain, which were discovered during a deep-sequencing analysis of oocyte's transcriptome. Thus, during my master thesis research, I cloned these isoforms from mouse oocytes and analysed their impact on miRNA and RNAi-like pathways in cultured cells. Using luciferase reporter system, I have found out that ectopically expressed short Argonautes do not affect miRNA and RNAi-like pathways suggesting that they are not functioning as dominant negative inhibitors of RNA silencing.

Keywords:

Argonaute, RNA silencing, miRNA, siRNA, RNA interference, oocyte, isoform, RISC

Table of contents

List of figures

Glossary

aa	amino acid
AGO	Argonaute protein
DGCR8	Di George Critical Region 8
DICER	RNAse III family endoribonuclease
ESCs	Embryonic stem cells
FL	firefly luciferase
MID	Middle domain – in AGO structure binds 5' end ribonucleotide base and phosphate group of guide short RNAs
MZT	Maternal to zygotic transition
nt	nucleotide
PAZ	PIWI, Argonaute and Zwille – protein domain binding 3' terminal ribonucleotide of short single-stranded RNAs
PIWI	p-element induced wimpy testes – AGO domain slicing target RNAs. Contains DEDH catalytic motif and coordinates two Mg^{2+} ions
Poly-A	polyadenylat –ion/-ed
RISC	RNA induced silencing complex
miRISC	miRNA RISC
RL	*Renilla* luciferase
RNAi	RNA interference
dsRNA	double-stranded RNA
ssRNA	single-stranded RNA
Small RNAs	
miRNA	micro RNA, genome-encoded small RNA
piRNA	Piwi interacting RNA
siRNA	short interfering RNA
TNRC6	Trinucleotide Repeat Containing 6 - GW182 family
ZGA	Zygotic genome activation

Single letter amino acid abbreviations

A – Alanine, C – Cysteine, D – Aspartic Acid, E – Glutamic Acid, F – Phenylalanine, G – Glycine, H – Histidine, I – Isoleucine, K – Lysine, L – Leucine, M – Methionine, N – Asparagine, P – Proline, Q – Glutamine, R- Arginine, S – Serine, T – Threonine, V – Valine, W – Tryptophan, Y - Tyrosine

Single letter abbreviation for nucleobases

A **–** Adenine, C – Cytosine, G – Guanine, T – Thymine, U - Uracil

1 Introduction

Argonaute family proteins carrying small RNA molecules form the core effector complexes executing RNA silencing. RNA silencing is a general term used for mechanisms employing small RNAs to repress viruses, mobile genetic elements, or genes (reviewed in Ketting 2011). A small RNA "guide" navigates the effector complex to complementary RNA molecules in a sequence-specific manner. The function of the effector complex is determined by the catalytic activity and identity of a specific Argonaute family protein, its binding partners, and by the type of non-covalent interaction of a small RNA with its target. Gene expression is regulated by RNA silencing on different levels; different Argonaute proteins were shown to mediate repression at the level of transcription as well as translation, or to induce degradation of messenger RNAs (reviewed in Fabian & Sonenberg 2012, Ketting 2011, Wilson & Doudna 2013).

Recent findings implicate Argonaute homologues in innate immune responses against foreign nucleic acids also in Bacteria and Archaea; in contrast to the eukaryotic Argonautes, some of their prokaryotic counterparts can provide host organisms with the protection against exogenous DNA molecules and plasmids (reviewed in Claycomb 2014, Swarts et al. 2014). A wide spectrum of recent small RNA-mediated mechanisms in eukaryotes has presumably evolved from ancient prokaryotic defence mechanisms.

The first discovered small RNA mechanisms was RNA interference (RNAi), which is typically induced by the double-stranded RNA (Fire et al. 1998). Most of RNA viruses and many endogenous mobile elements produce double stranded RNA (dsRNA) intermediates as a part of their replication cycle. Indeed, dsRNA, which is rarely present in eukaryotic somatic cells, serves as a common pathogen marker and triggers various defence mechanisms in affected cells (reviewed in Gantier & Williams 2007). One of them is RNAi initiated by an RNase Dicer, which recognizes dsRNA and cleaves it into short RNA duplexes (Bernstein et al. 2001), which are subsequently loaded on Argonaute proteins (AGOs). AGOs select one strand of the duplex (called short interfering RNA – siRNA) and use it as a guide for the recognition of complementary viral RNAs. Targeted RNA molecules are then sliced by the AGO's endonucleolytic PIWI domain. Remaining RNA fragments are degraded by cytoplasmic exonucleases, while complex of AGO with small RNA (called RISC

– RNA induced silencing complex) is available for targeting of another complementary RNA (reviewed in Tanguy & Miska 2013, Wilson & Doudna 2013).

Antiviral RNAi is used by many invertebrates and plants (reviewed in Ding & Voinnet 2007), but it is rarely active in mammals (reviewed in Cullen et al. 2013). Importantly, mammalian somatic cells respond to the exogenous dsRNA by a potent, sequence-independent interferon response which shuts down cellular metabolism to prevent viral replication (reviewed in Gantier & Williams 2007, Reynolds et al. 2006). Accordingly, mammalian cells do not efficiently process dsRNA by the RNAi machinery, with the noticeable exception of the oocytes and possibly also ES cells which lack interferon response (reviewed in Sagan & Sarnow 2013). RNAi is essential for the oocyte maturation and subsequent early embryonic development likely because of its contribution to the repression of mobile genetic elements (reviewed in Svoboda 2014).

Another RNA-silencing mechanism to be found in mammals is the piRNA pathway guarding the genome against mobile genetic elements mainly in the germline (reviewed in Siomi et al. 2011). Argonautes from the PIWI subfamily associate with distinct group of small RNAs called PIWI-interacting RNAs – piRNAs (Girard et al. 2006). The name "PIWI" comes from *Drosophila* mutant phenotype "p-element induced wimpy testes" (Lin & Spradling 1997, Pal-Bhadra et al. 2002). piRNAs are produced in a Dicer-independent manner from genome-encoded single-stranded RNA (ssRNA) precursors and are substantially different from other mammalian small RNAs (reviewed in Han & Zamore 2014). PIWI proteins not only cleave mRNAs transcribed from mobile elements, but also induce epigenetic silencing (Kuramochi-Miyagawa et al. 2008) of genomic loci coding for them in the nucleus (reviewed in Han & Zamore 2014, Weick & Miska 2014). piRNA pathway is presumably acting in the synergy with RNAi against transposons in mouse oocytes, but oocyte maturation and early embryonic development are not compromised in the absence of PIWI proteins. The opposite situation exists in the male germline; males lacking any of three PIWI proteins are sterile because of defected spermatogenesis (Carmell et al. 2007, Deng & Lin 2002, Kuramochi-Miyagawa et al. 2004).

While PIWI pathway and RNAi have rather defensive roles and are active only in a few specific cell types in mammals (reviewed in Siomi et al. 2011, Svoboda 2014), the third RNA silencing mechanism called micro RNA (miRNA) pathway plays wide regulatory roles

in most cells (reviewed in Bartel 2009). It is the dominant mammalian RNA silencing mechanism affecting gene expression of a large fraction of genes. It is estimated that up to 80% of all genes is regulated in total by miRNAs (Friedman et al. 2009, Grosswendt et al. 2014, Lewis et al. 2005). miRNAs are ~21 nt long small RNAs produced from genome-encoded hairpin precursors in the nucleus. These precursors are typically processed by Dicer in the cytoplasm and are loaded on one of four mammalian Argonaute proteins (AGO1-4). Unlike RNAi which relies on the AGO2 catalytic activity (in mammals), miRNA charged RISC induces an indirect translational repression and mRNA degradation rather than a direct endonucleolytic cleavage. The main reason is that miRNAs are usually not perfectly complementary to their targets which is a prerequisite for the AGO2-mediated target cleavage (reviewed in Bartel 2009, Shenoy & Blelloch 2014). Moreover other three AGO2 paralogs lost their catalytic activity in the course of evolution (Nakanishi et al. 2013, Schürmann et al. 2013, Swarts et al. 2014). Indeed, indirect repression of targeted transcripts requires several Argonaute cofactors; among them GW182/TNCR6 protein family has a crucial role (reviewed in Fabian & Sonenberg 2012).

miRNA and RNAi pathways virtually merge at the stage of Dicer-processing and are hardly distinguishable in their silencing outcomes, because the pool of small RNAs is shared among all four mammalian *Ago* paralogs (reviewed in Bartel 2009). Three catalytically-inactive mammalian AGOs work in the miRNA-like mode, while only AGO2 can induce direct cleavage of perfectly complementary target RNAs (Liu et al. 2004, Meister et al. 2004). Sorting of specific short RNAs to different AGOs has been reported, but association is generally random and proportional to ratios of available Argonaute proteins (Burroughs et al. 2011, Czech & Hannon 2011).

Mammalian Argonaute proteins are likely involved in other processes beyond the posttranscriptional regulation of gene expression. Emerging nuclear functions, including transcriptional and epigenetic regulation well-known from plants and invertebrates, were reported recently also in mammals (reviewed in Cecere & Grishok 2014, Huang & Li 2014, Meister 2013). However, a direct transcriptional silencing remains controversial (for discussion see Cullen et al. 2013, Svoboda 2014). As my research was focused on post-transcriptional regulation, I will not review these new functions in further detail in my thesis.

Considering contribution of miRNAs to virtually any complex biological process, it is surprising that canonical miRNAs are completely dispensable for oocyte maturation and preimplantation development of mouse embryos (Ma et al. 2010, Suh et al. 2010). While Dicer and active RNAi pathway are essential for oocyte maturation and progression through meiosis (Bernstein et al. 2003, Flemr et al. 2013, Kanellopoulou et al. 2005, Murchison et al. 2005, 2007; Stein et al. 2015), the miRNA pathway is largely inactive and functionally unimportant (Ma et al. 2010, Suh et al. 2010). Why mouse oocytes tolerate non-functional miRNA pathway and what causes its natural inactivation is still an enigma.

Interestingly, we discovered truncated Argonaute transcripts in deep-sequencing data of the oocyte transcriptome. This led us to test whether short Argonaute proteins encoded by these transcripts could have any impact on miRNA pathway. We hypothesised that these isoforms, which encode only the Argonaute N-terminal domain, could squelch important Argonaute cofactors (i.e. GW182) and in this way inhibit the cofactor-dependent miRNA pathway while leaving RNAi pathway unaffected.

1.1 Biogenesis of siRNAs

As already mentioned, siRNAs are generated from long dsRNAs by RNase III nuclease Dicer (Bernstein et al. 2001, Knight & Bass 2001). The mammalian Dicer processes dsRNA into short RNA duplexes 21 - 23 nucleotides long with 2 nucleotides (nts) overhangs on 3' ends (Bernstein et al. 2001). However, long dsRNA is present in somatic mammalian cells rarely under normal circumstances. RNAi is ineffective even in the presence of exogenous dsRNAs of viral or experimental origin in the cytoplasm. There are two main reasons. First, processing of dsRNA molecules by the somatic mammalian Dicer is rather slow compared to the processing of pre-miRNA (Flemr et al. 2013). Second, other dsRNA recognizing proteins like Toll-like receptor-3 or cytoplasmic protein kinase R (PKR) trigger the IR and TGF-β signalling leading to the cell-cycle arrest, inhibition of translation essentially overriding antiviral RNAi, and eventually, apoptosis (reviewed in Wang & Carmichael 2004). Nonetheless, some mammalian cell types such as oocytes and stem cells have the IR switched off and RNAi readily detectable (Li et al. 2013b, Maillard et al. 2013, reviewed in Sagan & Sarnow 2013, Svoboda 2014).

Oocytes and ES cells deal with endogenous dsRNAs generated by three different mechanisms: (i) by the transcription of inverted repeats, (ii) by convergent (bidirectional) transcription i.e. from transposons, (iii) or by pairing of sense mRNAs with antisense transcript of cognate pseudogenes *in-trans* (Flemr et al. 2013, Tam et al. 2008, Watanabe et al. 2006, 2008). Pseudogenes, transposons and inverted repeats are typically epigenetically silenced in somatic cells, but convergent transcription occurs regularly. However, negligible amounts of endogenous siRNAs detected in somatic cells suggests that endogenous dsRNA is not efficiently cleaved by Dicer and that siRNAs are not functionally relevant in these cells (Flemr et al. 2013).

1.2 Biogenesis of miRNAs

Biogenesis of miRNAs starts with transcription of long, genome-encoded miRNA precursors called primary miRNAs (pri-miRNA) by RNA polymerases II (Lee et al. 2004). Pri-miRNAs have the characteristic short hairpin structure typically containing a few non-complementary (or "bulged") nucleotides in the ~35-bp long stem region and a loop on top of the stem. The hairpin is flanked by longer unstructured RNA stretches. Some pri-miRNA transcripts contain more short hairpins (reviewed in Kim et al. 2009). These flanking regions are trimmed in the nucleus by the microprocessor complex composed of RNase III Drosha (Lee et al. 2003) and its essential cofactor DGCR8/Pasha, which binds the loop in the pri-miRNA hairpin structure. In fact, DGCR8 physically brings Drosha to its substrates (Gregory et al. 2004, Han 2004, Yeom et al. 2006). Similarly to Dicer, Drosha also generates 2-nt overhang on the 3' end of processed pri-miRNAs. This structural feature is recognized by the PAZ domains of both Dicer and Argonaute downstream in the miRNA pathway (Kim et al. 2009). Resulting hairpin pre-miRNA is exported to the cytoplasm by exportin-5 (Yi et al. 2003) for further processing by Dicer which removes a loop from the pre-miRNA producing miRNA duplex with characteristic 2-nt overhangs at 3' ends (Bernstein et al. 2001). The matured miRNA duplex is loaded to one of four mammalian Argonautes forming so called miRNA induced RISC – miRISC.

1.3 Function of siRNAs – RNA interference

The mammalian RNAi pathway refers to siRNAs loaded on AGO2, the only catalytically active mammalian AGO (Liu et al. 2004, Meister et al. 2004), to seek and directly cleave cognate RNA molecules of viral or endogenous origin (reviewed in Wilson & Doudna 2013). This interpretation of RNAi stems from the initial discovery made by Andrew Z. Fire and Craig C. Mello, who were awarded the Nobel prize in Physiology and Medicine in 2006 for describing RNA interference as a sequence-specific mRNA degradation induced by long dsRNA (Fire et al. 1998).

AGO2 cleaves only perfectly complementary RNAs at the position corresponding to the middle of the guide siRNA between nucleotides 10 and 11 (measured from 5' end of the guide)(Rivas et al. 2005, Schwarz et al. 2004). This process is catalysed by AGO2 PIWI domain which positions two Mg^{2+} ions to destabilize backbone phosphate of targeted RNA in a similar manner as RNase-H does (Rivas et al. 2005, Schirle et al. 2014, Schwarz et al. 2004). The reaction mechanism generates 5'-phosphate and 3'-hydroxyl termini in released RNA products (Schwarz et al. 2004). Only AGO2 PIWI domain, unlike other mammalian *Ago* paralogs, contains complete DEDH catalytic tetrade – four spatially

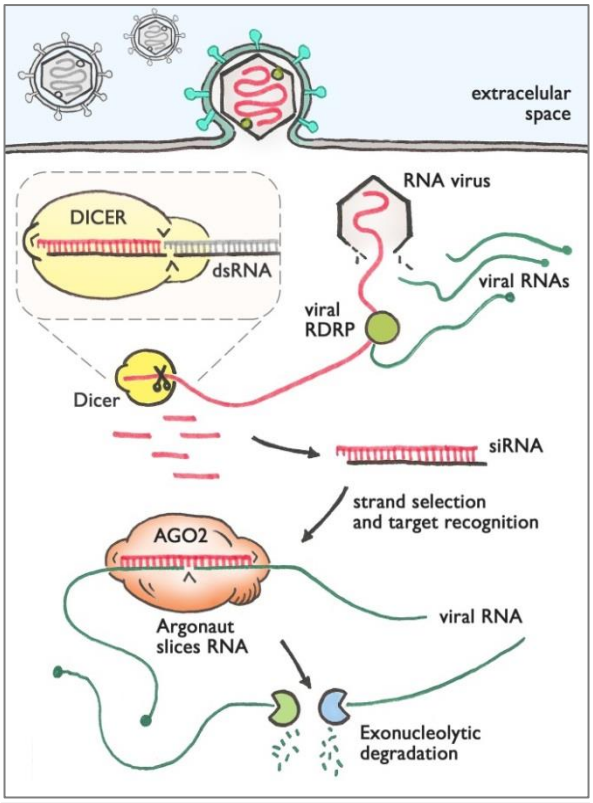

Figure 1 – antiviral RNA interference
Long dsRNAs of viral or experimental origin present in the cytoplasm are recognized and processed by Dicer into short ~21 nucleotides long short interfering RNA duplexes. Argonaute proteins select one strand from the duplex RNA and use it as a guide sequence to search for complementary viral mRNA molecules. AGO2 slices viral RNA in the case of perfect complementarity with the guide sequence. Argonaute then dissociates and seek for another target molecule. Fragments of viral RNA are degraded by cytoplasmic exonucleases i.e. XRN1. This mechanism allows for efficient degradation of viral intermediates preventing viral replication. Endogenously produced dsRNAs originating from bidirectional transcription, pseudogenes or long hairpin transcripts are processed in the same way.

organized residues necessary for the cleavage (Elkayam et al. 2012, Nakanishi et al. 2013, Schirle et al. 2014, Schirle & MacRae 2012). Adoption of the catalytically competent conformation requires that the 3' end of the guide strand is released from the PAZ domain allowing for a formation of a guide-target double-helix. siRNA target sites are often located within open-reading frames (ORFs) of mRNAs (reviewed in Ameres & Zamore 2013), but siRNAs are generally rare in mammalian somatic cells and do not seems to play any important role neither in the gene-regulation nor in antiviral defence. Notable exceptions from the rule are mouse oocytes (Svoboda et al. 2000, Wianny & Zernicka-Goetz 2000) and embryonic stem (ES) cells (Babiarz et al. 2008, Billy et al. 2001, Kanellopoulou et al. 2005) where active RNAi pathway was detected (described in a more detail in the Chapter 0).

Nonetheless, two recent studies have reported functional antiviral RNAi in mammals (Li et al. 2013b, Maillard et al. 2013). Li and colleagues reported effective RNAi response against insect Nodamura virus (NoV) in suckling mice (not in adult) and in hamster cells (Li et al. 2013b). RNAi was effective only against NoV lacking RNAi suppressor B2 (Li et al. 2013b). In the other study Maillard et al. infected mouse ES cells with encephalomyocarditis virus and detected siRNAs of viral origin loaded on AG02 (Maillard et al. 2013). The observation of active RNAi in suckling mouse suggests that antiviral RNAi may work also in mammals, but rather under specific circumstances or in certain cell types. It is plausible that the mammalian germline and somatic stem cells which can't be easily replaced might prefer RNAi to IFN in antiviral defence, because they must avoid the IFN-induced apoptosis. Mammalian antiviral RNAi still remains highly controversial topic (for discussion see reviews Cullen et al. 2013, Svoboda 2014, Tanguy & Miska 2013).

Interestingly, kinetic analysis showed that mouse AGO2-RISC is adapted for miRNA-mediated repression rather than for direct cleavage of mRNAs, as dissociation rate constant for seed-matched and fully complementary targets is similar (approx. 0.5 ms). This value is 90-fold larger than for *Drosophila* AGO2-RISC which is optimized for target cleavage. In mouse, a perfectly complementary target is as likely to be cleaved as to dissociate and can probably often escapes before slicing even occurs (Wee et al. 2012).

1.4 Function of miRNAs

Mammalian miRNAs have important roles in cell differentiation, ontogenesis, cell maintenance and homeostasis, as well as in response to various extra- and intracellular stimuli (reviewed in Ameres & Zamore 2013, Bartel 2009, Pauli et al. 2011, Shenoy & Blelloch 2014, Svoboda & Flemr 2010). miRNAs induce translational repression and mRNA degradation (Guo et al. 2010) and thereby precisely tune protein levels in cells (Baek et al. 2008, Selbach et al. 2008). miRbase – a web database of annotated miRNAs - contains almost 1,193 miRNAs for mouse and 1,881 high confidence miRNAs for Human – miRBase v. 21 (retrieved 1.5.2015) (Kozomara & Griffiths-Jones 2014).

Considering, that a single miRNA can regulate dozens or even hundreds of genes, it is challenging to predict biological outcomes of miRNA regulation networks (Friedman et al. 2009, Grosswendt et al. 2014, Gurtan & Sharp 2013). Taken together, the majority of mammalian genes is likely regulated by miRNAs in certain cellular or physiological context (Friedman et al. 2009, Grosswendt et al. 2014, Helwak et al. 2013, Lewis et al. 2005).

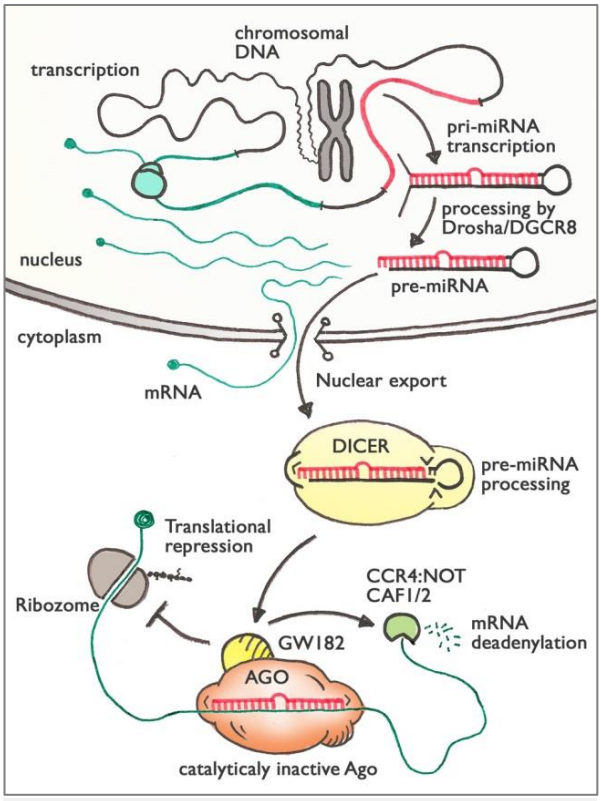

Figure 2 – miRNA Pathway
miRNAs are produced in the nucleus from genome encoded short RNA-hairpins by microprocessor complex composed of RNase Drosha and its cofactor DGCR8. pre-miRNA is exported from the nucleus by Exportin-5 (not shown) for processing by Dicer. Dicer removes the loop from miRNA precursor and forwards miRNA duplex to one of Argonaute family proteins. One miRNA strand drives Ago binding to partially complementary target sites in mRNA molecules. miRNA-mediated RNA silencing requires Ago cofactor from GW182/Tnrc6 family which interacts with deadenylation complexes CCR4:NOT and PAN2/3. Deadenylation results in translational repression followed by decapping and RNA degradation.

1.4.1 Targeting by miRNAs

The so called "seed" is a short sequence on the 5' end of a guide miRNA located between guide nucleotides g2 and g7 used for target-binding – Fig. 3 (Elkayam et al. 2012, Lewis et al. 2003, Schirle & MacRae 2012, Wee et al. 2012). The complementarity between miRNA seed and target mRNA (seed-target) is sufficient for the induction of silencing effects and was thought to be a prerequisite for active miRNA targeting (Baek et al. 2008, Guo et al. 2010). Accordingly, the 5' end of metazoan miRNAs is the most evolutionary conserved part of their sequence (Friedman et al. 2009). Recent experiments revealed that 80% of all miRNAs regulate their targets just through the seed sequence with no need for more extensive base-pairing (Grosswendt et al. 2014, Helwak et al. 2013). Theoretically, given hexa- or hepta-nucleotide combinations can be found in dozens and even hundreds of mammalian transcripts allowing the cell to regulate a whole set of genes by the expression of a single miRNA (Baek et al. 2008, Friedman et al. 2009, Grosswendt et al. 2014, Helwak et al. 2013, Lewis et al. 2005).

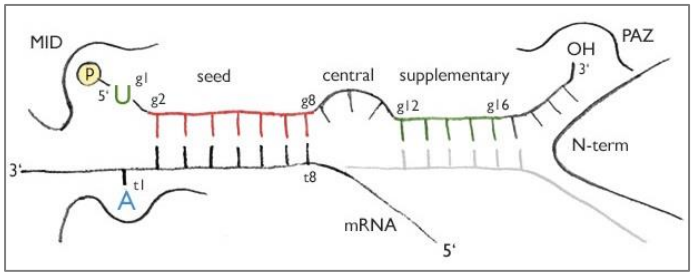

Figure 3 – miRNA Structure and Targeting
Typical miRNA is 21-nt long and is bound via the first 5' uridine monophosphate (yellow) in the MID and via two last 3' nucleotides in the PAZ domains of Argonaute protein. Majority of miRNA-target interactions are carried out by the base-pairing in the "seed region" (red) localized between nucleotides g2-g7 in the sequence of guide miRNA strand. Corresponding sequence in the mRNA is called "seed-target". Target binding is greatly enhanced by the presence of t1 adenine nucleotide (blue). Some miRNA targets exhibit extended complementarity in the "supplementary region" corresponding to nucleotides g12-g16 (green). The base-pairing beyond the nucleotide g17 is hindered by protruding portion of the N-terminal domain. Pairing in the central region and the release of 3' end is necessary for the cleavage of perfectly complementary targets by Ago2.

The strongest silencing effect is achieved when the seed-pairing is supported by an extended complementarity with the guide-nucleotide g8 and by the presence of t1 adenine in the target sequence (Bartel 2009). T1 adenine is preferred by a selective binding pocket within the Argonaute structure (Schirle et al. 2014). Importantly, the first 5' guide nucleotide (g1) does not contribute to the specificity of the miRNA target recognition because it is sequestered within the MID domain and thus unavailable for base-pairing. Surprisingly, target-binding

to nucleotides g9 and g10 decreases binding affinity (Schirle et al. 2014), in concordance these two positions are not well conserved in vertebrate miRNAs (Lewis et al. 2005). RISC binding can be further enhanced by guide-target interactions in the "supplementary region" localized between nucleotides g13-g16 (Bartel 2009, Wee et al. 2012). As already mentioned, AGO2-mediated cleavage requires extensive complementarity especially in the central region of miRNA. Any dinucleotide mismatch between nucleotides g7 and g12 completely abrogates endonucleolytic cleavage (Liu et al. 2004, Meister et al. 2004, Wee et al. 2012).

Recent studies revealed, that approximately 40% of functional miRNA-target interactions contain one or two mismatches in the seed region in human HEK293 cells (Helwak et al. 2013). The same phenomenon was detected also in *C. elegans,* mouse and human cell lines (Grosswendt et al. 2014). Such non-canonical interactions were often supported by additional base-pairing in the supplementary region. These studies showed that miRNAs mismatching at positions g2 or g7 are still able to silence their targets. This makes comprehensive *in silico* prediction of miRNA-target sites practically impossible (Grosswendt et al. 2014) and points-out to the inevitable off-targeting effects in knock-down experiments, which are caused by miRNA-like behaviour of experimentally used siRNAs. Even "seedless" interactions (16% of all detected guide-target crosslinks) are still able to induce moderate silencing of targeted transcripts (Helwak et al. 2013). These observations erode the common perception of miRNA targeting modes presuming perfect complementarity between the seed and seed-target (Bartel 2009, Grosswendt et al. 2014, Helwak et al. 2013). miRNA target sites are thought to be localized mainly in the 3' untranslated region (3'UTR) of mRNAs. However, some studies reported that over 40% of physically detected interactions between miRNAs and their targets maps into open reading frames in human (Helwak et al. 2013) and mouse (ES) cells (Leung et al. 2011). Our perception of the miRNA targeting will have to be updated if these observations are confirmed.

1.4.2 miRNA activity is GW182 dependent

The miRNA-mediated RNA silencing does not require AGO slicing activity, but relies on the essential Argonaute cofactor from the GW182/TNRC6 protein family (Eulalio et al. 2008, Liu et al. 2005a). GW182 proteins function as a scaffold for additional effector complexes which execute translational repression and mRNA degradation – Fig. 4 (reviewed in Fabian & Sonenberg 2012, Guo et al. 2010).

AGO PIWI domain contains two pockets binding tryptophan residues from the N-terminal domain of GW182 – Figure 11B, page 40 (Pfaff et al. 2013, Schirle & MacRae 2012). The C-terminal "silencing domain" of GW182 contacts CNOT9 and weakly also CNOT1 - two subunits of a CCR4:NOT deadenylation complex, which truncates poly-A tail of the miRISC target mRNAs (Behm-Ansmant et al. 2006, Chen et al. 2014, Mathys et al. 2014). A similar interaction has been reported for another deadenylation complex PAN2:PAN3 (Christie et al. 2013). It is still unclear to what extent are these two complexes redundant (reviewed in Fabian & Sonenberg 2012). RNA silencing is enhanced by the interaction between the GW182 silencing domain and poly-A binding proteins (PABP). This interaction ensures that miRISC-associated deadenylases get close to their poly-A substrate (Zekri et al. 2013).

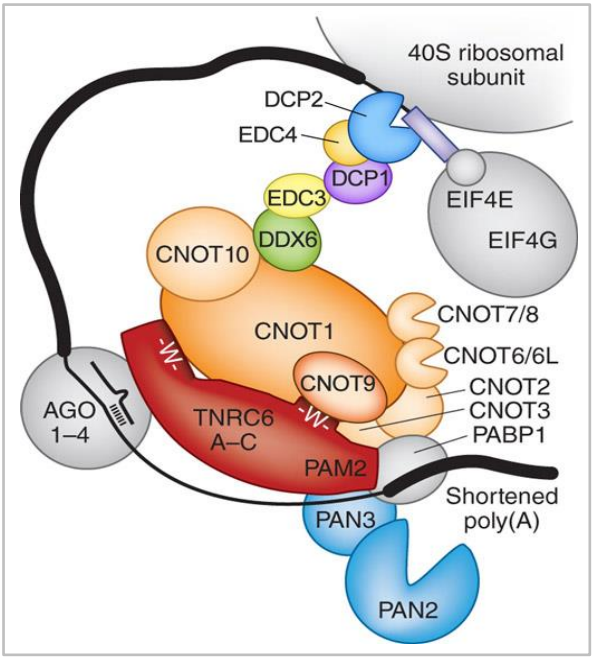

Figure 4 – RISC-CCR4:NOT complex.
Main interacting partner of Argonaute is GW182/TNRC6 family protein (red) which functions as a scaffold for deadenylation complexes CCR4:NOT (orange) and PAN2/3 (blue). GW182 binds to Poly-A binding proteins (PABP1 - grey) and in this way tethers the RISC to mRNAs. The core CCR4:NOT component CNOT1 functions as a hub for other factors executing translational repression, mRNA deadenylation, decapping and decay. Among those ATPase DDX6 (green) works as an inhibitor of translational initiation and also physically couples the deadenylation executed by CNOT7/8 and CNOT6/6L components with the decapping complex DCP1/2 (violet, blue). miRNA-mediated repression is initiated by the displacement of PABP proteins resulting in the loss of the mRNA loop structure. This is followed by the deadenylation and later by decapping. mRNA decapping requires enhancers of decapping EDC4 and EDC3 which links DDX6 with DCP1 subunit. Decapping triggers exonucleolytic mRNA decay (not shown). GW182 as well as deadenylation and decapping complexes are necessary for efficient repression induced by miRNAs. Adapted from Hafner et al., 2011 according to Mathys et al., 2014 and Chen et al., 2014

1.4.3 Translational repression induced by miRNAs

mRNA stability and rate of translation directly correlate with the length of poly-A which is bound by PABPs (reviewed in Sonenberg & Hinnebusch 2009). PABPs protect mRNA from exonucleolytic degradation and play essential role in the translation initiation by interacting with translation initiation factor eIF-4G, which binds the 5'-7-methyl-guanosine cap-associated factor eIF-4E. This complex, together with other initiation factors, closes mRNA into a loop structure and recruits ribosomes for translation (reviewed in Fabian & Sonenberg 2012). miRISC induced mRNA deadenylation prevents binding of PABPs to the poly-A tail and thus disallows translation initiation. The component of CCR4:NOT complex protein CNOT1 plays the crucial role in mRNA silencing providing many binding sites for other enzymes. It directly interacts and activates an abundant DEAD box ATPase DDX6, which then slows down elongation and initiation of translation (Chen et al. 2014, Mathys et al. 2014). It has been reported that PABPs are firstly removed from poly-A tail by the (direct or indirect) action of CNOT1 and CNOT6 components of CCR4:NOT complex even in absence of deadenylation (Zekri et al. 2013). This observation attributes translational repression to the dissociation of PABPs resulting in the loss of the closed loop mRNA structure (Zekri et al. 2013). Deadenylases must first get the end of the poly-A tail to their catalytic site in order to shorten them; therefore PABPs must be displaced, because they would otherwise sterically hinder the reaction. If PABPs are essential for translational initiation, then not only deadenylation but also their displacement inhibits translational initiation. In any case, non-translated mRNAs are ultimately deadenylated, which marks them for subsequent degradation (revieved in Fabian & Sonenberg 2012).

1.4.4 mRNA degradation induced by miRNAs

Degradation of deadenylated, non-translated and destabilized mRNAs is initiated by DCP2-mediated decapping (Behm-Ansmant et al. 2006). Several reports have shown that DDX6 recruits DCP2, therefore physically links deadenylation complex with the decapping machinery - Fig. 4 (Chen et al. 2014). This conclusion is in concordance with observations that miRNA silencing requires both deadenylation and decapping complexes (Behm-Ansmant et al. 2006). The mRNA decapping is followed by the 5'-to-3' XRN1 exonucleolytic

degradation. Deadenylated mRNAs are also degraded from the 3′ end by the exosome complex (reviewed in detail in Ameres & Zamore 2013, Fabian & Sonenberg 2012).

A recently described cascade of molecular interactions downstream of GW182 (Chen et al. 2014, Christie et al. 2013, Mathys et al. 2014) provides mechanistic explanation for the miRNA-mediated RNA silencing. The interacting network is highly complex, often redundant, robust, and difficult to delineate. Regardless of the precise molecular mechanism, miRNA silencing results in specific down-regulation of mRNA and protein levels (Baek et al. 2008, Guo et al. 2010, Zekri et al. 2013).

1.4.5 P-bodies

Argonaute protein often localize into so called GW-bodies or processing (P) bodies, which appear as bright cytoplasmic foci containing proteins acting in RNA metabolism (Jakymiw et al. 2005, Liu et al. 2005a,b; Pillai et al. 2005, Sen & Blau 2005). P-bodies are complex ribonucleoprotein structures with variable composition and size implicated in translational repression and in several RNA degradation pathways including general mRNA decay, nonsense-mediated decay, and miRNA-induced degradation (reviewed in Decker & Parker 2012). P-bodies completely lack ribosomes or translation initiation factors (except of eIF4-E stably associated with 5’ mG cap) forming translationally silent environment with enhanced RNA degradation activity (reviewed in Leung & Sharp 2013).

Depletion of GW182, DDX6 or LSM1-7 proteins (components of exosome) results in P-body loss and inhibition of miRNA-activity (Jakymiw et al. 2005, Liu et al. 2005a). Many proteins involved in RNA degradation and translational repression have been reported to localize into PBs, among them noticeably Argonaute proteins, CCR4:NOT complex, decapping complex DCP1:DCP2, XRN1 exonuclease, helicase DDX6 and many others (reviewed in Decker & Parker 2012, Leung & Sharp 2013). These observations suggested that PBs may play significant role in RNA silencing.

Localization of miRISC-bound RNAs into P-bodies likely enhances their degradation and can serve as an indicative microscopic hallmark of active miRNA pathway. However microscopically detectable PBs are not necessary for miRNA silencing as only approx. 1% of all present AGO2 localizes into PBs in HeLa Cells (Leung & Sharp 2013). New superresolution microscopy techniques should reveal dynamics of these multiprotein complexes in the future.

As miRISC dissociates from target molecules very quickly and moves inside the cell cytoplasm close to the rates of the free diffusion (Wee et al. 2012), I speculate that RISC must form relatively stable complexes with both deadenylation and decapping proteins to have any chance to induce target repression. In other words, efficient miRNA silencing requires certain threshold concentrations of all factors involved. Here comes the advantage of subcellular compartments like P-bodies, which increase local concentration of related factor by multitude of mutual interactions, enabling such a complex molecular mechanism to be carried out. This idea is consistent with the notion that only a few most abundant miRNA species actually induce measurable target silencing in cells (Broderick & Zamore 2014, Wee et al. 2012).

1.5 Argonautes – the core of RISC

Argonaute protein family has evolutionary conserved PIWI and AGO subfamilies engaged in different biological processes (reviewed in Meister 2013). All mammalian Argonaute family members share the same architecture having four highly conserved protein domains and size around 850 amino acids. The structure of Argonautes exhibits a bilobal architecture with N-terminal and PAZ (PIWI-Argonaute-Zwili) domains forming one lobe and MID (middle) and PIWI domains forming the other one (Figure 5). Two linkers L1, L2 between N-PAZ and PAZ-MID domains form the bottom of the cleft and function as a hinge between the lobes.

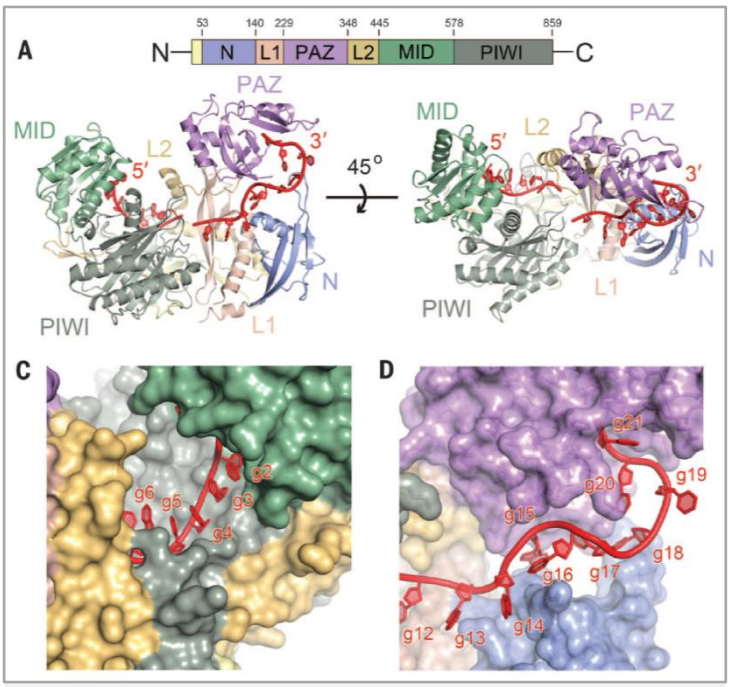

Figure 5 – Structure and domain organization of human AGO2

A – Colours of individual domains in the crystal structure (cartoon) correspond to the domain scheme above (numbers indicate aa residue on domain borders). hAgo2 adopts a bilobal fold with MID and PIWI domains (left) and PAZ and N-terminal domains (right) forming the two lobes. Guide RNA is shown in red. C – Bases g2-g5 are exposed to the solvent for initial scanning of target RNAs. D – 3' portion of guide is buried inside the narrow N-PAZ channel unavailable for base-pairing. Adopted from Schirle et at., 2014

The small RNA is stretched in the central cleft between the two lobes anchored by its 3' hydroxyl group in PAZ domain and with first 5'-nucleotidephosphate in a pocket within the MID domain. The first guide nucleotide (typically uridine-monophosphate) stacks to the aromatic ring of Y529 which also forms hydrogen bond with 5' phosphate (Frank et al. 2010, Schirle & MacRae 2012). First and last two guide nucleotides are therefore inaccessible for target-binding. Despite that, mammalian miRNA target-sites often begin with t1 adenine. Its presence in the recognized sequence substantially enhances binding-affinity (Schirle et al. 2014) and contributes to stronger silencing effects (reviewed in Ameres & Zamore 2013, Bartel

2009). This is explained by the presence of adenine-selective pocked between L2 and MID domains in the structure of human AGO2 (Schirle et al. 2014).

Guide nts g2 to g5 (from 5' end) are exposed into the solvent in A-like helical conformation prepared to scan available cytosolic RNAs for potential target sites (Fig. 5C), while the rest of the guide sequence remains sequestered inside the cleft (Fig. 5D)(Schirle et al. 2014, Schirle & MacRae 2012). Upon the binding of target RNA to nts g2-g5, AGO undergoes conformational change allowing for further pairing with nts g6-g8 and also with "supplementary region" corresponding to g13-g16 (Schirle et al. 2014).

Mammalian catalytically active AGOs likely adopt yet another conformation allowing for the cleavage of a target RNA. This probably involves releasing the 3' end of the guide strand from the PAZ domain, thus allowing for the formation of RNA double helical structure and repositioning of scissile residues in the active site (Schirle et al. 2014).

1.5.1 Argonaute loading with small RNAs

Both siRNAs and miRNAs produced by Dicer are loaded specifically on one of four mammalian AGO subfamily protein members. The precise mechanism of the AGO loading is not yet completely understood, but several facts are already known. First, loading of short RNA duplex is promoted by the action of chaperone HSP90 (Johnston et al. 2010). HSP90 helps AGO protein to adopt an open conformation in which short RNA duplex can be positioned in to the RNA-binding cleft. Moreover, HSP90 markedly improve stability of empty AGOs (Johnston et al. 2010). However, purified AGOs can be effectively charged with single-stranded short RNAs as well as with short duplexes in the absence of any supplementary proteins *in vitro* (Deerberg et al. 2013).

Identity of the 5' terminal nucleotide together with thermodynamic stability at 5' ends (less stable is preferred) determines which strand will be retained and used for targeting (Khvorova et al. 2003, Schwarz et al. 2003). The other strand is called "passenger" or "miRNA*" and it must be displaced for full activation of the RISC. Passenger strand displacement is an ATP-independent process (Czech & Hannon 2011). Once passenger strand is released, 3' end of the guide strand is bound by the PAZ domain.

1.5.2 Unclear functions of the AGO N-terminal domain

The N-terminal (N) domain is of paramount interest for our research; because all short Argonaute isoforms mentioned previously stretch over the entire N-domain and terminate farthest in the N-portion of PAZ domain.

The N-domain was shown to spatially prevent guide-target duplex propagation beyond nucleotide g16 in the structure of *Thermus thermophiles* (Wang et al. 2009). A very similar domain arrangement can be found in structures of human Argonautes suggesting, that guide nucleotides g18-g21 are inaccessible for pairing (Elkayam et al. 2012, Schirle et al. 2014, Schirle & MacRae 2012). Accordingly guide-target mismatches corresponding to nucleotides g17-g20 have negligible impact on the target-binding (Wee et al. 2012). Yet these observations do not elucidate functional importance of N-domain.

Recent domain swapping experiments and redesigning of catalytically inactive human Argonautes (AGO1, AGO3 and AGO4) into slicing enzymes helped to identify protein regions required for target cleavage. Indeed, an intact catalytic DEDH core within the PIWI domain is necessary but, surprisingly, not sufficient for cleavage (Faehnle et al. 2013, Hauptmann et al. 2013, Schürmann et al. 2013). AGO3 contains functional PIWI domain but remains catalytically inactive.

Two short N-terminal motives localized between amino-acids 44-48 (M1) and 134-166 (M2) of hAGO2 were identified to be necessary for effective target slicing. hAGO3 is inactivated by mutations in the M1 motive and by the bulky insertion of eight aa in the M2 motive, which protrudes near to the catalytic PIWI-core and thus hinders proper positioning of catalytic residues (Schürmann et al. 2013). Detailed examination identified critical role of methionine 47 for target slicing (Kwak & Tomari 2012, Schürmann et al. 2013).

The N-domain seems to have regulatory role as it is positioned proximate to the PIWI catalytic core. Several groups proposed a role of N-domain in the proper positioning of the guide-target complex for slicing and in the cleavage and/or unwinding of passenger strand from small RNA duplex to active AGO (Faehnle et al. 2013, Hauptmann et al. 2013, 2014; Kwak & Tomari 2012, Schürmann et al. 2013).

Activation of catalytically inactive Argonautes is possible only when they are loaded with miRNA duplexes containing several mismatches (bulges). Then, passenger strand is displaced passively by-slicer independent mechanism; it dissociates as AGO forms more

extensive contacts with guide strand decreasing binding energy within the RNA duplex. Passive unwinding is accelerated by proposed “wedging” activity of the N-terminal domain (Kwak & Tomari 2012). Perfectly complementary siRNA duplexes can be employed only by AGO2, which can resolve passenger strand; in this way binding energy between the two strands is minimized and remaining fragments of passenger strand can dissociate. Surprisingly M47 necessary for target-slicing is dispensable for passenger strand displacement. This suggests that process of passenger strand-splicing and displacement is different from target-slicing. Motif M2 is required for efficient RISC activation (unwinding of siRNA duplexes), while M1 is required for target-slicing. But presence of both is required for full activity of AGO2 and for turning on AGO3 slicing capacity (Faehnle et al. 2013, Hauptmann et al. 2013, Schürmann et al. 2013).

1.6 Mouse oocytes: a unique case of RNA silencing

Mammalian gametes and early embryos are unique in many regards including the fact that they contain all three types of small RNA species. The miRNA pathway, dominant RNA silencing mechanism in somatic cells, is iactive in mouse oocytes, while piRNA and RNAi pathways are active (reviewed in Svoboda & Flemr 2010). A stable environment in oocytes, which supports stockpiling of maternal factors, is accompanied by elevated activity of mobile genetic elements (MGE). Random integration of these elements into coding or regulatory regions of the genome may cause irreversible damage and is therefore controlled by RNAi and piRNA pathways. Active RNAi in oocytes can be, in part, attributed to the absence of interferon response and to the presence of sufficient amounts of dsRNA. Lack of the interferon response in oocytes and ES cells allows injecting the long dsRNA to manipulate gene expression with RNAi (Stein et al. 2003, Svoboda et al. 2000, Wianny & Zernicka-Goetz 2000).

1.6.1 The piRNA pathway

As mentioned earlier, the piRNA pathway guards the genome against a potentially harmful integration of MGS in the germline (reviewed in Weick & Miska 2014). In mice, three PIWI proteins (MILI, MIWI, and MIWI2) associate with a piRNAs, which guide them to target complementary RNAs (Aravin et al. 2006, Girard et al. 2006). All mouse PIWI members are catalytically active and can cleave target RNAs with perfect complementarity to the piRNA guides (De Fazio et al. 2011, Reuter et al. 2011). Mammalian piRNAs substantially differ from miRNAs and siRNAs in their biogenesis, chemical structure and length; they are 26-30 nt long and have characteristic 2'-O-methylated ribose at the 3' end. These features, together with common 5' uracil, drive their loading exclusively to the PIWI subfamily of Argonautes (Aravin et al. 2006, Girard et al. 2006). Biogenesis of piRNAs is Dicer-independent and lacks any double-stranded RNA substrate, which is typical for the production of siRNAs (reviewed in Han & Zamore 2014). It was demonstrated that piRNAs repress transcription of mobile genetic elements, induce epigenetic silencing of transposon containing loci in the nucleus (Kuramochi-Miyagawa et al. 2008), and also cause degradation of RNA intermediates at post-transcriptional level (De Fazio et al. 2011, Reuter et al. 2011). Functional piRNA pathway is essential for the spermatogenesis and male fertility in mice (Carmell et al. 2007, Deng & Lin 2002, Kuramochi-Miyagawa et al. 2004).

Although piRNAs represent around 46% of all short RNA reads in mouse oocytes –Figure 6 (García-López et al. 2014), The piRNA pathway is not required for the oocyte maturation and early embryonic development (Carmell et al. 2007, Deng & Lin 2002, Kuramochi-Miyagawa et al. 2004). The highly active RNAi pathway in mouse oocytes has been predicted to compensate for the lost function of the PIWI proteins in knockout females (see further below). It is unclear whether the same phenotype can be expected in other mammals outside of the *Muridae* family (Flemr et al. 2013).

1.6.2 RNAi in mouse oocytes

Mouse oocytes and zygotes contain substantial amounts of endogenous siRNAs (endo-siRNAs) comprising over 30% of all RNA in cells – fig. 6 (García-López et al. 2014). Endo-siRNAs are generated from long dsRNA precursors derived mainly from retrotransposons in Dicer-dependent manner (Murchison et al. 2007, Tam et al. 2008, Watanabe et al. 2006, 2008). Complete loss of the *Dicer* gene resuplts in lethality at around embryonic day 8; moreover, numbers of homozygous embryos even in earlier stages of development does not correspond to the normal Mendelian ratio for heterozygous mating (Bernstein et al. 2003). Females with conditional elimination of Dicer early in oocyte development are sterile and exhibit severe defects in meiosis I, explaining the deviation from the Mendelian laws by haploinsufficiency (Murchison et al. 2007, Tang et al. 2007). Transcriptome of *Dcr*$^{-/-}$ oocytes is dramatically perturbed, with almost 20% of all genes

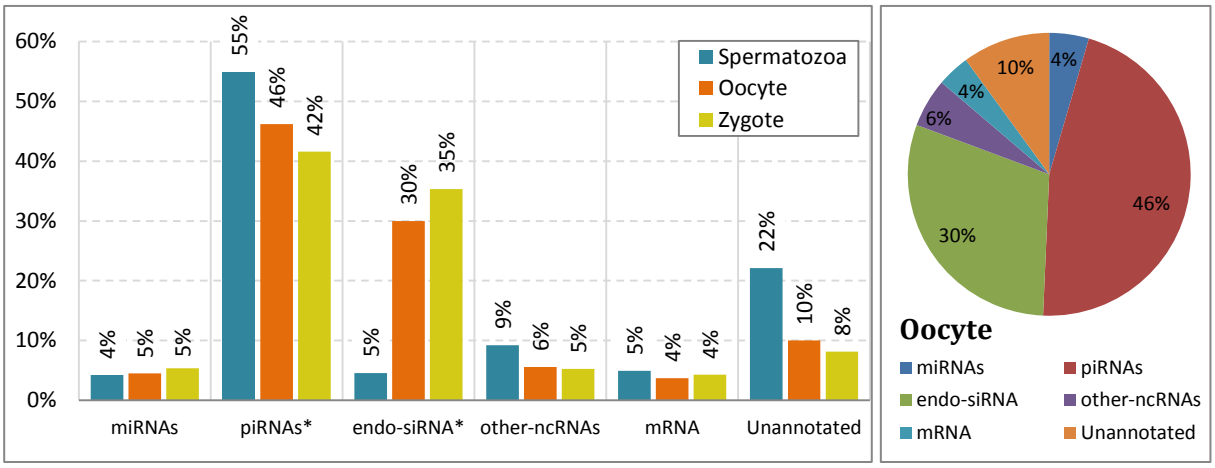

Figure 6 - Relative abundance of deep-sequencing reads in mouse gametes and zygote
Data from García-López et al., 2014, Ilumina sequencing, only short 18-32 nt reads shown. Total: 34 million short reads from spermatozoa and over 50 million reads from ~1500 oocytes and zygotes, respectively. Relative distribution of reads is shown as a pie chart on the right.

missregulated and elevated expression of mouse transcripts (MT) retrotransposons and SINE MGE (Flemr et al. 2013, Murchison et al. 2007, Tang et al. 2007). Our group has recently described a truncated Dicer isoform characteristic for mouse oocytes (Dicer^{O}) which processes dsRNAs much more effectively than the full-length somatic Dicer. Transcription of Dicer^{O} is driven from an MT insertion, which works as an alternative oocyte-specific promoter. Deletion of this insertion results also in meiotic defects and female sterility (Flemr et al. 2013), thus phenocopying complete Dicer knockout. The same phenotype was reported for oocyte-specific conditional knockouts of *Ago2* (Kaneda et al. 2009, Lykke-Andersen et al. 2008) and recently also for catalytically inactive AGO2 knock-in mice (Stein et al. 2015), but not for knockouts of other mouse Argonaute genes (Stry et al. 2012). This suggest an evolutionary pressure[1] to retain enzymatic activity of at least one mammalian Argonaute paralog. Taken together, these observations point out to the importance of functional and effective RNAi pathway in mouse oocytes.

1.6.3 Inactive miRNA pathway in mouse oocytes

Remarkably, described meiotic phenotype and female sterility after the conditional deletion of *Dicer* or *Ago2* was initially attributed to the lack of functional miRNA pathway (Kaneda et al. 2009, Murchison et al. 2007, Suh et al. 2010, Tang et al. 2007).

Fully-grown germinal vesicle oocytes (GV) are transcriptionally silent and contain large amount of maternally provided proteins and mRNAs. These factors orchestrate oocyte-reprograming into a totipotent zygote during meiotic maturation and after the fertilization (so called maternal-to-zygotic transition - MZT). Most of maternally provided factors are degraded before the activation of embryonic genome in the 2-cell stage (reviewed in Li et al. 2013a, 2013, Svoboda & Flemr 2010, Walser & Lipshitz 2011). miRNAs were initially thought to contribute to the clearance of maternal transcripts during MZT (Suh et al. 2010, Tang et al. 2007). Indeed, their contribution for transcript-clearance has been shown in vertebrates, such as *Danio* and *Xenopus* (Giraldez et al. 2006, Lund et al. 2009). However, the knockout of mouse *Dgcr8* gene showed that mutant oocytes lacking canonical miRNAs can support development to the term. Moreover, transcriptome of

[1] Another explanation for conserved Ago2 catalytic activity in mammals brought the discovery of a dicer-independent but Ago2-slicer dependent biogenesis pathway which generates miR-451 essential for erythropoiesis (Cheloufi et al. 2010).

DGCR8-deficient oocytes is practically indistinguishable from that of wild-type oocytes (Suh et al. 2010). These observations demonstrate that canonical miRNAs do not play a critical role in the oocyte maturation, nor in the degradation of maternal transcripts during MZT. Importantly, miRNAs are required later for post-implantation development where they contribute to the cell differentiation and organogenesis (revieved in Carroll et al. 2013, Pauli et al. 2011, Shenoy & Blelloch 2014).

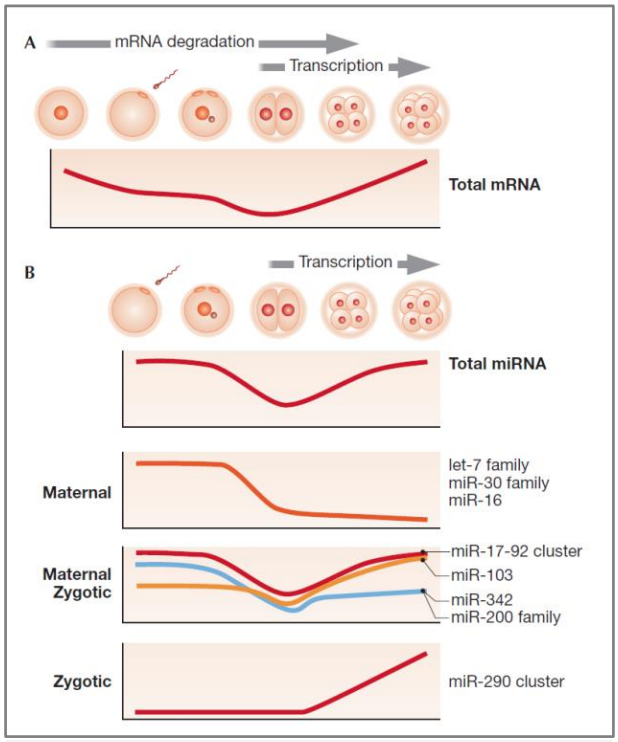

Figure 7 – mRNA and miRNA dynamics in maternal to zygotic transition in mouse.
A - mRNA abundance during the oocyte maturation (fully grown GV oocyte, MII egg) through the fertilization (middle - zygote) and embryonic growth to the 8 cell stage. Embryonic transcription is launched in the two cell stage in mouse. B – miRNAs follow a similar pattern, but the major wave of degradation occurs between the zygote and two-cell stage. Different miRNA classes exhibit different patterns of regulation. Adopted from Svoboda & Flemr, 2010

Most of miRNAs present in the oocyte undergo similar degradation as coding transcripts reaching the lowest levels in the two-cell embryo – Figure 7. Increase in the miRNA abundance during early development is concomitant with activation of the embryonic genome (Murchison et al. 2007, Tang et al. 2007). A recent deep-sequencing analysis showed that miRNAs represent only ~5.5% of all RNA reads in oocytes and zygotes (García-López et al. 2014). Considering that miRNAs compete with 7x more abundant siRNAs for binding to the same Argonautes, it may not be surprising, that miRNA function is partly disrupted.

Our group and others have previously showed that even the most abundant maternal miRNAs in oocytes belonging to miR-30 and Let-7 families (Murchison et al. 2007) have reduced capacity to repress translation of injected luciferase reporters containing corresponding target sites in their 3'UTR (Ma et al. 2010) – Figure 8A-D. Importantly, an extent of reporter-repression by corresponding miRNAs gradually decreases as oocyte

grows (Ma et al. 2010). Correspondingly, P-bodies (the hallmark of the active miRNA regulation) are detectable in small meiotically incompetent oocytes but disappear as oocyte reach the size of ~50 μm – Figure 8E (Flemr et al. 2010).

P-body loss and apparent suppression of miRNA activity can be inflicted by the change of the oocyte volume resulting in altered stoichiometry between available Argonautes and their cofactors, or/and miRNAs and their target sites in the increased pool of maternal transcripts accumulated during the oocyte-growth.

Alternatively, ineffective translational repression of miRNA targets might be caused by a qualitative change in miRISC or in associated factors. Candidates for such a qualitative

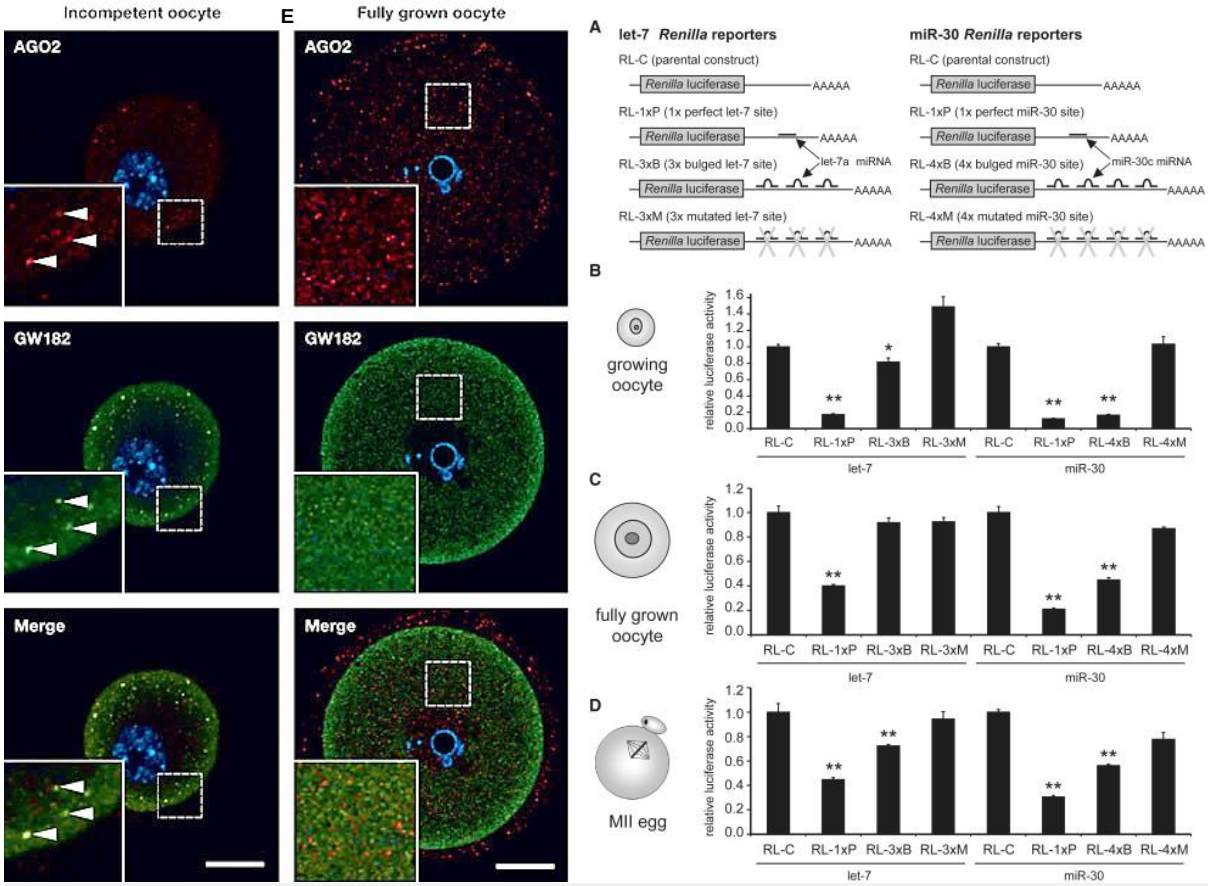

Figure 8 – Suppressed activity of the miRNA pathway in mouse oocytes

A) Scheme of the *Renilla* luciferase reporter plasmids, which have Let-7 or miR-30 miRNA target sites in the 3'UTR. Perfect (RL-P) reporters reflect activity of RNAi-like pathway, while bulged (RL-B) reporters contain target sites with central nucleotides in the target sites mutated, thus reflect activity of the miRNA pathway. B-D – Performance of reporters in different stages of oocyte development. Bulged reporters are not effectively repressed in GV and MII oocytes (Adopted from Ma et al., 2010). E) P bodies (yellow foci in overlaid image) are lost in fully grown oocytes (adopted from Svoboda & Flemr, 2010) –staining of Ago2 (red) and GW182 (green)

change are Argonaute proteins themselves, GW182 family proteins or some factors from CCR4:NOT complex. Correspondingly, our group previously observed that P-bodies are restored after the microinjection of GW182, but not AGO2 mRNAs, suggesting that GW182 is the limiting factor for the miRNA silencing in oocytes (M. Flemr – unpublished data). In any case, the molecular mechanism responsible for inactivity/suppression of the miRNA pathway in oocyte and early embryos remains unknows.

2 Aims of the project

The main aim of this thesis was to characterize short Argonaute isoforms, which encode only the N-terminal part of Argonaute proteins and are found in mouse oocytes. Their existence was first noticed in deep-sequencing data of RNA from fully-grown oocytes. My main task was to annotate, clone and functionally analyse short Argonautes in order to test whether they have any impact on the miRNA pathway.

To address this question, my work included several essential subtasks:

1. Bioinformatic analysis including AGO isoform annotation and primer design
2. Cloning of AGO isoforms into expression vectors and validation of protein expression in cultured mammalian cells
3. Calibration of a luciferase reporter system for monitoring miRNA and RNAi activities in cultured cells
4. Functional analysis of ectopically expressed short AGO isoforms in cultured cells

In addition, we decided to generate an AGO2 deficient cell-line to have a positive control for effects of complete AGO2 elimination on the luciferase reporter system. We used a novel CRISPR/Cas9 nuclease technology in following three steps:

5. Design of short guide RNAs (sgRNA), which guided exon 2 deletion of the AGO2 gene by the CRISPR/Cas9 system
6. Development of a screening procedure for the detection of positive cell-clones
7. Production of AGO2-defficient cell line.

3 Material and Methods

3.1 Bioinformatics analysis

3.1.1 Deep-sequencing, annotation of cloned isoforms

cDNA libraries from mouse CB56Bl/6 oocytes, MII eggs and zygotes were amplified and deep-sequenced on the Illumina Ilx genome Analyzer and 35-nt single-end and 76-nt paired-end reads were mapped on the mouse genome assembly NCBI37/mm9 (Abe et al. 2015). Sample preparation and deep-sequencing was conducted by our colleagues in Japan and the data were mapped by Vedran Franke. The datasets are available in the ArrayExpress database under reference (Abe et al. 2015). Mapped data were visualised as a custom track online in the UCSC genome browser (http://genome-euro.ucsc.edu/). Sequencing results were mapped back on the mouse genome with UCSC BLAT function.

3.1.2 Structural modelling

Protein sequences of mouse maternal version of full-length Ago2 and maternal Ago3-B were uploaded for the homology based structural modelling on Phyre-2 web server with intensive mode option on (Kelley & Sternberg 2009). Flexible loop (aa 820-840) in the PIWI domain missing in the template crystal structure of human Ago2 (PDB ID: 4olb) was modelled on the FALC-Loop web server (Lee et al. 2010) of Seoul national university and the best scoring FALC (minimal free energy) loop conformation was used in the final structure of mAgo2 in the Figure 11. The surface potential of Ago3-B isoform was calculated on the APBS web server using default settings (Parse model)(Baker et al. 2001, Dolinsky et al. 2007) and solvent-accessible electrostatic potential (scale - ±10 kT/e) was projected on the surface of the modelled molecule in PyMol version 1.3 (Schrödinger).

3.2 Isolation of nucleic acids from mouse oocytes and tissues

Superovulated mouse females CD1xC57Bl6/J were primed with 150ul of the pregnant mare's serum gonadotropin (PMSG; 50U/ml, Polygon) 48 prior to the oocyte collection. Fully grown germinal vesicle (GV) oocytes arrested in the prophase of the meiosis-I were collected with mouth pipet into a droplet of the tempered M2 media (Sigma) supplemented with PDE3A phosphodiesterase inhibitor IBMX (3-isobutyl-1-methylxanthine; final [0.2 mM]; Sigma) preventing the resumption of meiosis. Oocytes were denuded from cumulus cells with tight glass pipet and washed in several M2-media

droplets to get rid of cumulus cells and ovarian-tissue debris before the final washing steps in the 1x PBS buffer. Clean oocytes were transferred in the minimal amount of PBS into a tube containing 0.5 µl of RiboLock - RNase inhibitors (Thermo Scientific; 40U/µl) in 5µl of RNAse free water and immediately frozen on dry ice and stored in -80 °C before further use.

Additionally, visceral organs from sacrificed mice were collected, quickly washed in PBS buffer, transferred into tubes and snap frozen in the liquid nitrogen. Later, suitable sized pieces of spleen, thymus or pancreas were homogenized in 0.5 ml of RNAzol RT (Sigma Aldrich), then 0.25 ml of RNAzol and 0.3 ml of RNase free water was added. Samples were mixed vigorously and spinned down at 12,000 RCF; 15 minutes. Supernatant was transferred into clean tubes and mixed with the equal amount of molecular grade isopropanol, mixed and incubated overnight at -20°C. Mixture was centrifuged at 12,000 RCF for 15 min in 4°C. Resulting pellet was washed twice with 0.5 ml of 75% molecular grade ethanol, and centrifuged at 10,000 RCF for 3 min. Dried pellet was dissolved in 30ul of RNase free water and samples were stored at -80°C for future applications.

3.2.1 Reverse transcription

The cDNA library was prepared directly from ~100 isolated GV oocytes without any RNA extraction steps. Oocytes in 5 ul of PBS were just mixed with 0.3 ul of RiboLock RNAse inhibitors and with 5 ul of H_2O; and heated 5 min at 85°C for the cell lysis. 1 ug of tissue RNA or lysed oocytes were used in reverse transcription reaction (20 ul) with the ReverseAid RT polymerase KIT (Thermo Scientific) performed according to the manufacturer's protocol (25°C, 10 min). Reactions were filled to 50ul with RNase free water and stored in -80°C.

3.3 Molecular cloning

3.3.1 PCR amplification of short *Ago* transcripts

Predicted Argonaute isoforms were amplified from cDNA samples from oocytes or tissues in a polymerase chain reaction (PCR) using the proofreading *Pfu* DNA polymerase (Thermo Scientific) with the following reaction setup:

10 x *Pfu* buffer + $MgSO_4$+	2.5 µl
12.5 mM dNTPs	0.5 µl (0.2 mM final)
10 uM Forward primer	1 µl (0.4 uM)
10 uM Reverse primer	1 µl
Template cDNA	1 µl
Pfu DNA polymerase (2.5U/µl)	0.5 µl
H_2O to the final volume of 25µl	18.5 µl

Program: 95°C – 5 min – initial denaturation, (95°C – 30s; 58°C – 30s; 72°C – 70s) - 30x, 72°C – 5 min. Samples were loaded on 1.5% agarose gel (LE Agarose - Lonsa) in and run in ~33 mM lithium bromide buffer (LB – pH8.5, 20x - 8.39g $LiOH{\cdot}H_2O$ + 36g H_3BO_4 in 1l H_2O) containing 0.1% ethidium bromide (Sigma). Following transcript-specific deoxyribonucleotide primers were ordered from Sigma Aldrich.

Mouse *Ago2*	
mAgo2-shortAC-F	5'-GCCTAAGAGAATCCTTCCTGCCTTCC-3'
mAgo2-shortA-R	5'-CAGTATGTGGTGGACTGTGGGTTGC-3'
mAgo2-shortC-R	5'-GAAGCAGGTAGTCTTGGGTTGCATAAGC-3'
Mouse *Ago3*	
mAgo3-ex1-F1	5'-GTCCGCTCCTCGCCTCTGTGG-3'
mAgo3-ex1-F2	5'-CCGACTGTGCCTCTTGTGCCC-3'
mAgo3-shortA-R	5'-TTCTGTGTGTGTGACGGTGTGTGC-3'
mAgo3-shortA-R2	5'-CACGCATGTGGCTACAGAGGCTC-3'
mAgo3-shortB-R	5'GGATGTCGTCACCTACTCTAATTGGTTTGG-3'

In the first round of the PCR with all possible primer combination only the *Ago2-C* was detected; other isoforms were detected in the following (semi)nested PCR reaction: 1st round was the same as previous reaction with the extension time 80s and annealing temperature increased to 60°C, 25 cycles. Reactions were diluted 10 times and 1 µl was used for the next round of PCR with inner primers (mAgo3-ex1-F2 + mAgo3-shortA-R2/mAgo3-shortB-R – semi-nested), 25 cycles otherwise the same as previous reaction.

Then bands of the expected size were excised from the gel and DNA was isolated with Gel extraction kit (Quigen) according to the manufacturer's protocol. Sample concentration was determined on the NanoDrop 1000 Spectrophotometer (Thermo Scientific).

3.3.2 Ligation, transformation and colony PCR

Short *Ago* transcripts from the mouse GV oocytes were ligated into the pJET1.2 plasmid (Thermo Scientific) with T4 DNA ligase (Thermo Scientific) according to manufacturer's protocol. 3 µl of ligation reaction were transformed to chemically competent Top10 *E. coli* bacteria (made in house; transformation reaction: bacteria were thawed on ice, incubated 20 min with ligation reaction, heat shock 42°C - 1 min, 5 min on ice, add 250 µl of LB media, shaking at 750 RPM for 1h at 37°C). Suspension of bacteria was plated on Amp^+ plates and grew overnight at 37°C.

Colonies were pre-screened with colony PCR reaction (0.5 µl of Taq polymerase, 2 µl of 10x Taq reaction buffer, 1.8 µl of 25mM MgCl2, 1 µl of each forward and revers 10 µM primer, 0.4 µl 12.5mM dNTPs, picked colony in 5 µl of H_2O, total volume 20 µl; program: 94°C 5min, 30 x (95°C - 30s, 58 °C – 30s, 72°C – 80s), 72°C – 5 min). Positive colonies were inoculated to 2.5 ml liquid LB media and cultured 12-16h at 37°C, 250 RPM. Plasmids were isolated with QuickLyse Miniprep kit (Quiagen) and plasmids were sequenced in GATC-biotech AG (Germany) – reaction was set up according to the company's instructions (500ng of plasmid DNA, 15 pM sequencing primer (pJET1.2_Rev2_seq) in total volume of 10µl).

pJET1.2_Rev2_seq 5'-CGGTTCCTGATGAGGTGGTTAGC-3'
pJET1.2_Fwd 5'- CGACTCACTATAGGGAGAGCGGC-3'

ORFs of *Ago2/3* transcripts were amplified from sequenced pJET1.2 plasmids with *Pfu* DNA polymerase (Thermo Scientic) with Fwd and Rev primers (Sigma-Aldrich) having terminal AgeI (ACCGGT) and NotI (GCGGCCGC) sites, respectively, for subsequent ligation into pSV40-cHA expression plasmid (Map in Supplementary information). Colonies were screened with the colony PCR as described earlier (with phRL-rev-seq – 5'-AGCAATAGCATCACAAATTTCAC-3' located in SV40 poly-A, and *Ago*2/3-AgeI-F primers) and positive clones were cultured overnight in 50 ml of liquid Amp^+ LB media for HiSpeed Plasmid MIDI kit (Quigen) isolation.

Ago2sAC-AgeI-F	5’-gatcACCGGTACCATGAGAGATAAGCTGAACTTTCTTGC-3’
Ago2sA-NotI-R	5´-ctagGCGGCCGCCGCGCCCTCATGAAGAAG-3’
Ago2sC-NotI-R	5’-ctagGCGGCCGCTTCATGCTTCTGCTCTTGCTTTG-3’
Ago3sAB-AgeI-F	5’-gatcACCGGTACCATGGAAATCGGCTCCGC-3’
Ago3sA-NotI-R	5’-ctagGCGGCCGCGAGGGGCTGACAAGACTGCTG-3’
Ago3sB-NotI-R	5’-ctagGCGGCCGCACCACAAGCTGAAAATTATCTTT-3’

Amplicons were re-cloned from pSV40-cHA into pCI/neo expression plasmid (Promega) digested with AgeI/MfeI (NEB1 buffer + BSA). Opened plasmid fragment was dephophorylated with SAP (Thermo Scientific) and extracted from gel. MfeI site is located in the middle of SV40-poly-A signal in both plasmids. HA-tagged *Ago*2/3 isoform were excised from pSV40-cHA vectors with AgeI/MfeI, gel-purified and ligated into dephosphorylated pCI/neo backbone. Resulting plasmids were isolated from 100ml of bacterial culture and verified by sequencing.

3.3.3 Construction of pSV40-cHA plasmid

This plasmid was constructed from pSV40-HA expression vector. 10 µg of plamid DNA was digested with AgeI, NotI (Thermo Scientific) restriction enzymes (CutSmart buffer). Reaction was loaded on gel and bigger product was isolated from gel in order to get rid of N-HA tag. Oligonucleotides (sigma) containing SalI-NotI-cHA were annealed in 50 µl reaction (1x T4 ligation buffer, 1 µl of each 100µM deoxyoligo, 5 min 95°C, gradually cooled down in switched off cycler) producing AgeI and degenerated NotI overhangs.

Sal-Not-cHA-F - ccggtaccatggtcgacattacgcggccgcagtacccatacgacgtcccagactacgcttgataa

Sal-Not-cHA-R – ggccttatcaagcgtagtctgggacgtcgtatgggtactgcggccgcgtaatgtcgaccatggta

Annealed duplex was ligated into AgeI/NotI pSV40-HA plasmid fragment, transformed and verified by sequencing. Original NotI site was lost. New pSV40-cHA plasmid (See plasmid map in Supplementary Information) allows for in frame insertion of ORFs with SalI/NotI generating C-terminally tagged proteins. AgeI/NotI cloning allows for the keeping of native N-termini in C-HA tagged proteins. This strategy was used for the cloning of mouse short *Ago*2/3 isoforms.

3.4 Cell culture and transfection

Mouse NIH3T3 cells and human HeLa cells were cultured in Dulbecco’s modified Eagle’s medium (DMEM) supplemented with 10% FCS, penicillin and streptomycin (Sigma) at 37°C in 5% CO_2 atmosphere. NIH3T3 or HeLa cells were plated on 24-well plates at the

density of 50,000 or 30,000 cells per well, respectively, 24 hours prior to the transfection in 0.5 ml of DMEM. Cells were transfected according to the manufacturer's protocol with TurboFect in vitro transfection reagent (Thermo Scientific) in the DNA[μg]:TurboFect[μl] ratio 1:1.5 or 1:2, respectively. Typically 500 ng of total plasmid DNA was transfected per well in 100 μl of serum-free DMEM. 8h later or next day, 1ml of DMEM with FCS was added in to each well. Cells were harvested 48h post-transfection for further analysis with an appropriate lysis buffer according to the subsequent use: Western blot or Dual luciferase assay (see below).

Anti-miR30c and anti-Let7 mixed antagomirs (Exiqon) were used for a specific inhibition of miR-30c and Let7 activity in HeLa cells. Impact on the miR-30 and Let-7 *Renilla* luciferase reporters was measured using dual luciferase assay described below (See Chapter 4.4. for detailed explanation of the reporter system used). To this end, antagomirs were co-transfected with plasmids encoding reporter luciferases with target sites of respective miRNA in their 3'UTR. For the transfection of a mixture of small antagomirs and reporter plasmids Lipofectamine 2000 transfection reagents (Thermo Scientific) was used according to the manufacturer's instructions.

3.5 Cell lysis for SDS-PAGE

Cells were collected into 2 ml of PBS, tubes were centrifuged at maximal speed for 1 min and supernatant was discarded. Cell lysis was performed with 200 μl of the lysis buffer containing 2x protease inhibitors cocktail set (Milipore) for 10-15 min on ice followed by centrifugation (15 min, 4°C, 12 000g). Collected supernatants were used for western blotting. **Lysis buffer:**

20 mM	HEPES (pH 7.8)
100 mM	NaCl
1 mM	EDTA (pH 8.0)
0.5%	IGEPAL CA-630 25% (Sigma-Aldrich)
1 mM	fresh DTT
0.5 mM	PMSF
1 mM	NaF
0.2 mM	Na3VO4

3.6 Western blot

Protein concentration in lysates was determined using standard curve of bovine serum albumin (BSA) in Bradford protein assay (Bio-Rad), absorbance was measured at 595 nm. Typically, the amount of a lysate corresponding to 40 μg of protein/per line was mixed with 5x loading buffer (0.2 M Tris, 20% glycerol, 10 mM β-mercaptoethanol, 1% w/v Bromphenol Blue, 10% w/v SDS). Samples were incubated 5-10 min at 95°C for denaturation, centrifuged for 1min at 8000 RCF and resolved on SDS-PAGE gel (12.5% separating gel, 7.5% stacking gel) with standard PageRuler Plus prestained Protein Ladder (ThermoScientific) at 100-150 V in 1x running buffer (10x - 0.25 mM Tris, 2 M Glycine, 1% SDS, pH ~ 8.8). PVVD membranes were activated in 100% methanol (30 s) and equilibrated in 1x semi-dry transfer buffer (10x - 12.5mM Tris, 96 mM Glycine). Classical sandwich assembly was placed into the semi-dry blotting apparatus and protein samples were transferred with 35 V for 50 min on the membrane. Membrane was removed from the sandwich and stabilized by 100% methanol for 30 sec, air dried and split into part for immunodetection of different proteins.

For immunodetection, membranes were then soaked in 100% methanol, equilibrated in 1 x TTBS buffer (150 mM NaCl, 10 mM Tris, 0.05% Tween 20, pH ~ 7.5), and blocked in blocking buffer (5% non-fat dry milk in 1xTTBS buffer) for 1 hour at room temperature (RT). Staining with anti-HA high affinity primary antibody (Roche, 11867423001, clone 3F10, rat) diluted 1:2500 in the blocking buffer was performed overnight at 4°C on a rocking platform. Next day, membranes were washed 3x for 5 min in blocking buffer and incubated with secondary goat anti-rat IgG (H+L), HRP conjugate antibody (Pierce, 31470) diluted 1:50,000 in blocking buffer, 1 hour at RT and washed 3x for 5 min in 1xTTBS buffer.

Then, membranes were incubated with a 0.5 – 1 ml drop of the Super Signal West Femto Maximum Sensitivity chemiluminescent substrate (Thermo Scientific) for one minute, excessive liquid was removed, and membranes were placed against the films in a dark room for time ranging from 30 s to 10 min.

3.7 Dual luciferase assay

Mammalian cells cultured on 24-well plates were transfected with pSV40 or pCI/neo expression plasmid encoding tested or control proteins (up to 500 ng), 25 ng of Firefly luciferase plasmid pGL4 (Promega) and variable amount of *Renilla* reporter plasmids (decribed previously in (Ma et al. 2010) as indicated above and in main text. Cells were harvested 48h post-transfection, washed with PBS, and lysed in 150 µl of PPBT lysis buffer (0.2 % v/v Triton x-100, 100 mM potassium phosphate buffer, pH 7.8). Cell lysates were cleared by a short centrifugation – 10,000 RCF for 1 min. 5 µl from each sample lysate was transferred on the 96-well Dynatec microflour 1 plate (white – Thermo Scientific) at RT while keeping already loaded wells covered to prevent evaporation. Luminescence of the samples were determined with Dual-Luciferase reporter Assay System (Promega; 40µl of both *Renilla* and Firefly substrate buffers used, 10s integration time) on the Modulus microplate Luminometer with dual injectors (Turner Biosystems).

The obtained luminescence values for *Renilla* luciferase reporters were normalized to values of non-targeted Firefly reporters expressed from the pGL4.10 plasmid. Values from triplicates were averaged and sample standard deviation was calculated. Further mathematical operations respected rules for the propagation of uncertainty. Results from independent experiments were averaged and SD was calculated as a square root from the sum of squared standard deviations from individual experiments.

3.8 Generation of *Ago2* knockout cell line with CRISPR/Cas9 nucleases

3.8.1 Design of sgRNAs

Sequence of the mouse *Ago2* gene was retrieved from genome assembly NCBI37/mm9 and sequences flanking the exon-2 were used as an input to the E-CRISPR (http://www.e-crisp.org/E-CRISP/) tool to identify best scoring target sites for sgRNAs. Based on the E-CRISPR output, 2 target sites in the inton-1 and 3 target sites in the intron-2 were selected. Exon-2 should be excised using a pair of sgRNAs resulting in the frameshift mutation. Sense and anti-sense oligonucleotides were ordered from Sigma-Aldrich.

sgRNA oligonucleotides:
Ago2-CR1-S - 5'-caccGAGGCCCAAGCCTCTCCAT-3'
Ago2-CR1-A - 5'-aaacATGGAGAGGCTTGGGCCTC-3'
Ago2-CR2-S - 5'-caccCACGCCCTTTGGATCCCG-3'

Ago2-CR2-A - 5‘-aaacCGGGATCCAAAGGGCGTG-3‘
Ago2-CR3-S - 5‘-caccCTGCCCCAGAGTTTTAGT-3‘
Ago2-CR3-A - 5’-aaacACTAAAACTCTGGGGCAG-3‘
Ago2-CR4-S - 5‘-caccACTATGTGACTTATGGTC-3‘
Ago2-CR4-A - 5‘-aaacGACCATAAGTCACATAGT-3‘
Ago2-CR5-S - 5‘-caccGTGGAACTATGTGACTTA-3‘
Ago2-CR5-A - 5‘-aaacTAAGTCACATAGTTCCAC-3‘

2µl of each 100µM sence and antisence oligonucleotides were annealed in 50µl of H_2O with 1x T4 ligation buffer, 5 min at 95°C in the cycler followed by a slow gradual cooling in the turned off machine. Oligonucleotides were phosphorylated with T4 kinase (Thermo Scientific) according to manufacturer’s instructions and ligated into BbsI linearized and dephosphorylated pPURO-U6-sgRNA plasmid (made in house by R. Malik). This plasmid contains two inverted BbsI sites, thus cleavage results in the overhangs ATGG and TTTG used for the directional cloning of annealed oligonucleotides. Plasmid contains remaining 5’ portion of the invariant sgRNA sequence under the U6 promoter. The insertion of an annealed oligonucleotide links invariant part with a variable portion of sgRNA used for the sequence specific targeting. Ligation, transformation, culture in bacteria, colony PCR screening, amplification in liquid LB and midi prep followed by sequencing were done as described earlier.

3.8.2 Production of clonal cell lines

NIH3T3 cells constitutively expressing spCas9 nuclease at high levels (clonal line #E8, made in house by R. Malik) were used for generation of *Ago2* knockout cell lines. To select the most active sgRNA combination, 100+100 ng of sgRNA pPURO-U6 plasmids supplemented with 300 ng of pBluescript DNA was transfected to the cells as described above. CR1+CR4 pair was identified as the most active combination in Touchdown PCR screening reaction (see results). This pair was used for generation of clonal cell lines. #E8 cells were plated at density of 40,000 cells/well and transfected next day as described earlier. After 24h, cells were washed with PBS, tripsinized and diluted for counting in the Bürker’s chamber. 100-200 cells were transferred on 15 cm dishes and culture for next 10-14 days at stable conditions till cell colonies reached a visible size. Colonies were transferred individually on the 24 well plates and expanded during the next week. As cells reached confluence, samples were collected for the isolation of genomic DNA for

genotyping and some cells were split on the new 24 well plate to keep the line in the culture. In the meantime, genomic DNA was isolated as described below and clones were genotyped. Positive clonal lines were expanded and stored in liquid nitrogen.

3.8.3 Isolation of genomic DNA

Cells were harvested after two day, washed with PBS and lysed in 400 µl of the "tail and liver" lysis buffer (0.1 M Tris, pH 8.5; 200 mM NaCl, 5 mM EDTA, 0.2% SDS) supplemented with 1 µl of proteinase K (>600U/mL, Thermo Scientific), shaking 250RPM at 55°C for 2h. 400µl of 100% molecular grade isopropanol was added, tubes were mixed by inverting. Precipitated genomic DNA was transferred into new tubes with a glass stick and dissolved in 300µl of H_2O, 10 min at 95°C for the inactivation of proteinase-K remains.

3.8.4 Genotyping of cell clones - Touchdown PCR

Genotyping was performed with primers designed to the exon-2 flanking introns. Typically, Touchdown PCR reaction was performed to reduce non-specificities.

mAgo2-ex2-F1: 5'-TTACCCGGCACTGGCACATACC
mAgo2-ex2-F2: 5'-AGAGAGAGGTGAAAGTCCCCAGC
mAgo2-ex2-R2: 5'-AGTGATGGAGAAGATGCCCAACG
mAgo2-ex2-R1: 5'-CCAGAGCAAGATAGATTAGCCCAGC

Primer combination F2+R2 was reliably used for genotyping:

		Program		
2 µl	10x Taq reaction buffer (Thermo Scientific)	95°C – 3:30 min		
1.6 µl	$MgCl_2$	95°C – 0:30		
1+1 µl	F+R primers 10 µM	72°C – 0:30	-1°C each cycle	10x
0.4 µl	15.5 mM dNTPs	72°C – 0:40		
2 µl	template DNA – typically 100-300 ng/µl	95°C – 0:30		
1 µl	Taq polymerase (Thermo Scientific)	60°C – 0:30		27-30x
11 µl	H_2O	72°C – 0:40		
		72°C – 4:00		

Possitive clones were werified by sequencing of isolated PCR products and used in the Dual Luciferase assay. See Results.

4 Results

4.1 Identification of short Argonaute isoforms in RNA deep-sequencing

This study was initiated by the discovery of novel unannotated Argonaute transcripts in RNA high-throughput sequencing (HTS) data from mouse fully-grown oocytes (Abe et al. 2015). We first noticed a few peaks in mapped HTS data not matching canonical *Ago* exons when browsing through mouse genes involved in miRNA pathway. A detailed analysis of the spliced reads in the polyadenylated (poly-A) fraction revealed two short transcript isoforms originating from the *Eif2c2* gene (*Ago2*) and a single isoform from the *Eif2c3* gene (*Ago3*) – Figure 10.

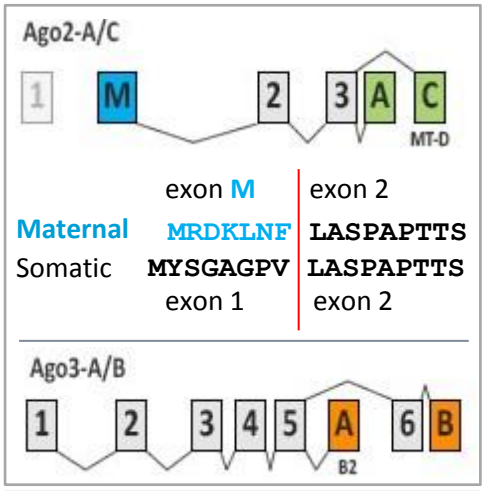

Figure 9 – Splicing scheme of short Argonaute transcripts. Maternal *Ago2* transcripts contain alternative first exon resulting in the change of the first 7 amino-acids on the N-terminus of resulting proteins.

Transcription of the maternal full-length *Ago2* and its isoforms starts from an alternative G-rich promoter located in the first *Ago2* intron. Splicing of the maternal exon1 (M) with standard exon2 results in AGO2 proteins with the first 7 N-terminal amino-acids altered – Figure 9. CF916663.1 mRNA from the fully-grown mouse oocyte deposited in the NCBI library also contains this maternal exon.

The first identified short transcript "*Ago2-A*" terminates right behind the exon 3 and the other one called "*Ago2-C*" terminates on an MT-D family LTR retrotransposon located in the intron 3 – Figure 9 and Figure 10A. We were not able to detect the end of the open reading frame (ORF) for another transcript called *Ago2-B*, which was predicted by splicing analysis (not shown).

We estimate that approximately 2/3 of all poly-A transcripts from the *Ago3* gene terminate in the intron 5 on a B2-SINE element. We designate this isoform corresponding to mRNA AK042049 (from neonate thymus) "*Ago3-A*". The DDBJ database contains another short *Ago3* mRNA AK172226 (from activated spleen) referred here as "*Ago3-B*" which terminates behind the exon 6 in the region highly conserved in mammals.

These isoforms apparently constituted most of poly-A transcripts originating from both genes suggesting a possible function in fully grown oocytes and zygotes. Moreover,

full-length *Ago2* and *Ago3* mRNAs were present in low levels in the poly-A fraction of the HTS data. *Ago1* and *Ago4* were practically absent in the oocyte transcriptome. These observations have been confirmed previously by other groups with quantitative PCR analysis suggesting higher abundance of *Ago3* compared to *Ago2* mRNA; but generally low levels of transcription (García-López & del Mazo 2012, Stein et al. 2015). In any case, the full-length *Ago2* must be present in oocytes in a sufficient amount supporting the highly active RNAi. Existence of annotated short Argonaute mRNAs and the discovery of novel putative transcripts in oocyte HTS data have prompted us to clone these isoforms for their functional analysis.

Figure 10 (on the next page): Annotation of mouse genes *Eif2c2* (*Ago2*) on chromosome 15 (A) and *Eif2c3* (*Ago3*) on chromosome 4 (B) retrieved from the UCSC genome browser (http://genome-euro.ucsc.edu/) with mapped RNA HTS reads (WE – whole extract) from mouse fully grown oocytes (GV – germinal vesicle), oocytes arrested in the metaphase of meiosis II (MII) and from 1-cell embryo - zygote (s_1cell) – data from Abe et al., 2015. Mapping of HTS data from GV oocytes published independently shows almost identical pattern – not shown (Smallwood et al., 2011). RefSeq Genes annotation of spliced exons marked as thick vertical lines (dark blue) with numbered exons. A) Ago2 transcription starts from an alternative maternal exon (M – light blue) in oocytes and zygotes. Most poly-A *Ago2* transcripts (not-shown) terminate on the alternative exon A and C in MII stage (green). B) Majority of *Ago3* transcript in MII eggs terminates on exon A, some also on the exon B (orange). Full-length poly-A transcripts for *Ago2* and *Ago3* are represented in MII egg by approx. 8 and 170 reads, respectively. Numbers in the top lines of A and B indicate genomic coordinates on the mouse genome assembly NCBI37/mm9 from July 2007. Note the different scale for mapped reads in A and B.

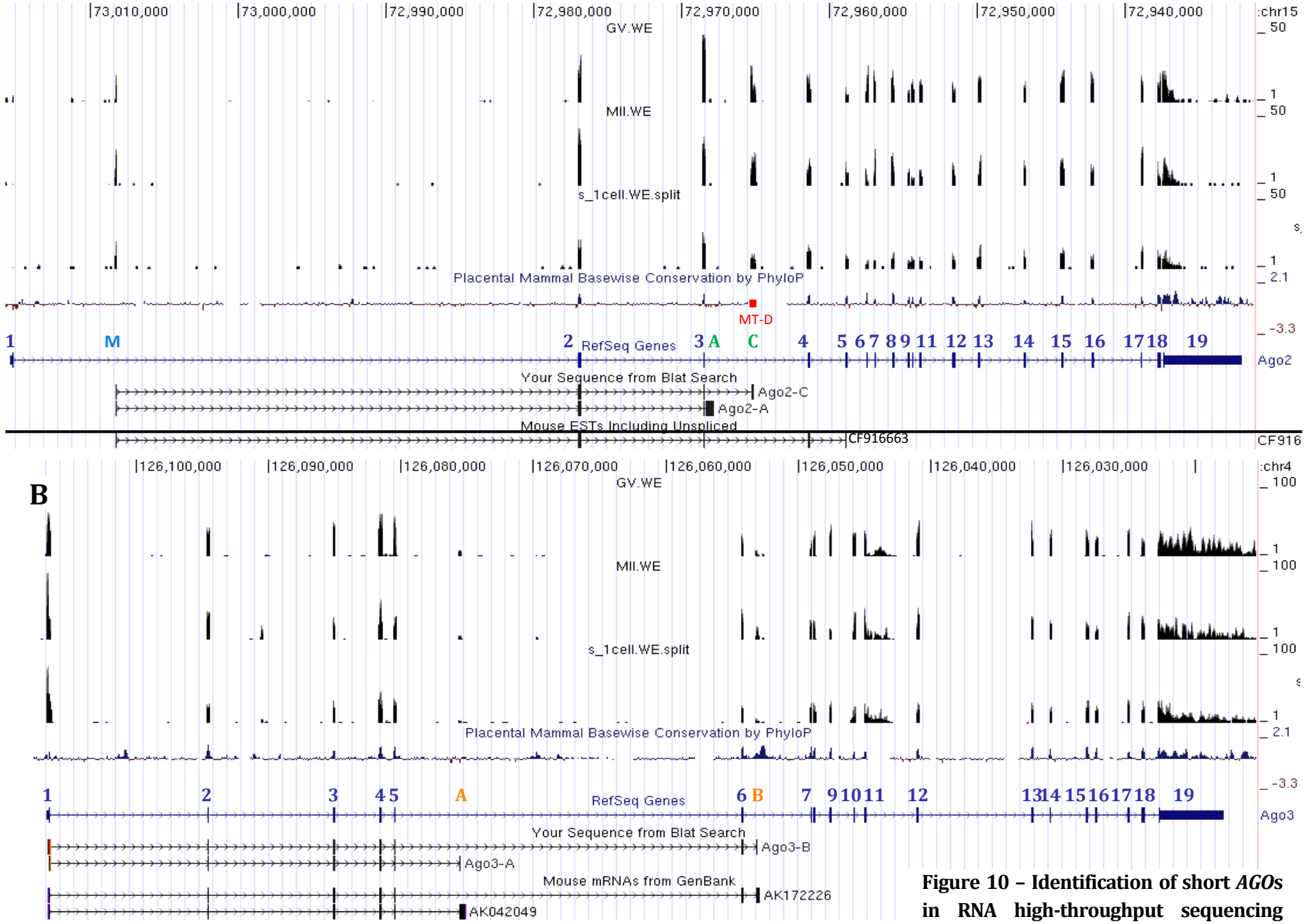

Figure 10 – Identification of short *AGOs* in RNA high-throughput sequencing

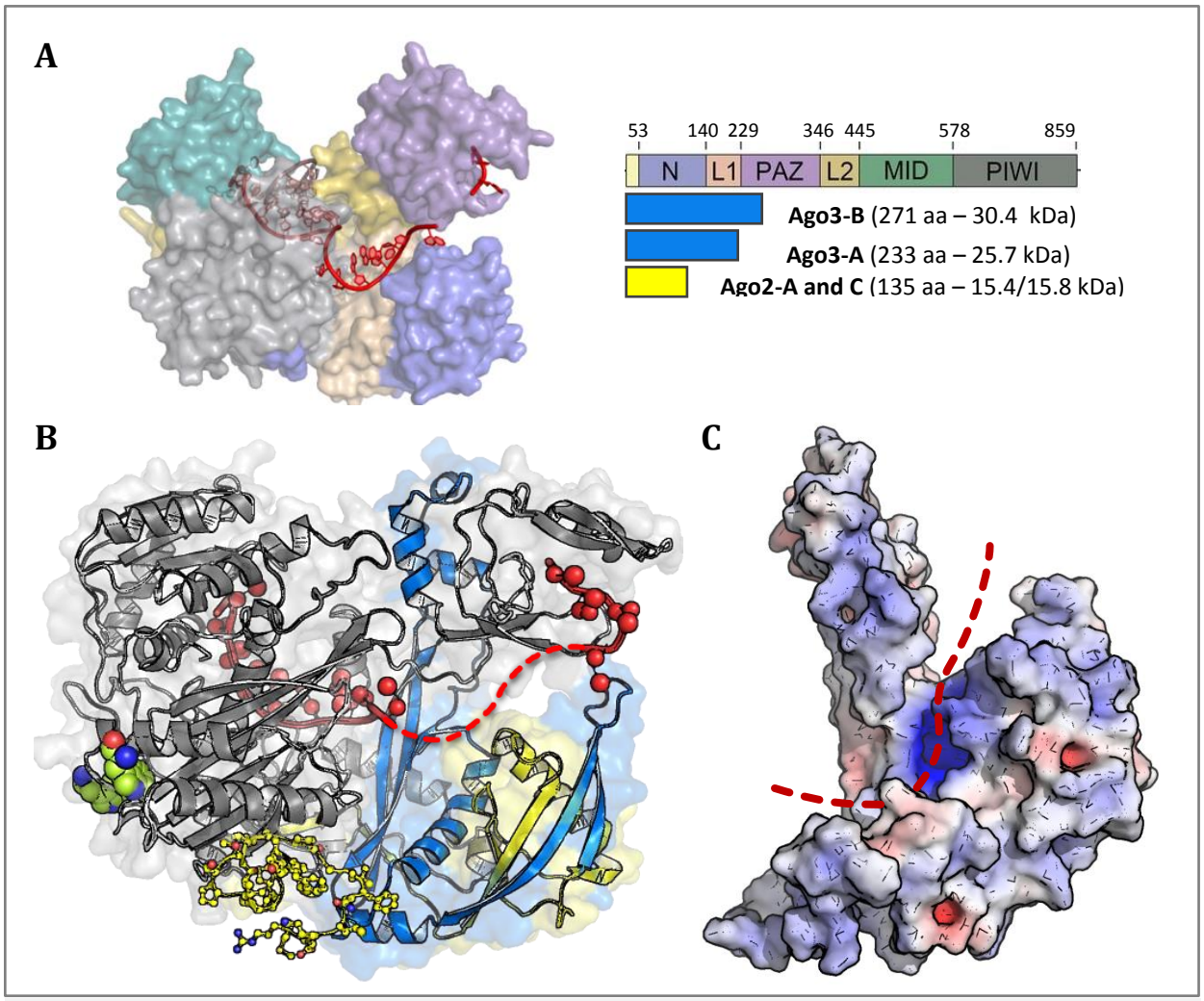

Figure 11 – Model of mouse Ago3-B.

A) The crystal structure of Human Ago2 with bound guide RNA and a short target (red) is colored according to colors used in the domain scheme in the top-right corner. Blue and yellow rectangles below the domain scheme correspond to the size of short Ago3 (blue) and Ago2 (yellow) isoforms from mouse oocytes (Schirle et al., 2014, PDB ID 4W5O). B) Modelled structure of full-length mouse Ago2 (blue and yellow) shows that this protein terminates in the first third of the PAZ domain and lacks pocket binding 3' end of the guide RNA. Disordered and likely highly flexible N-terminus (yellow balls & sticks) was modelled ab initio by Phyre-2 server. The two free tryptophans bound in the hydrophobic pockets on the surface of the PIWI domain are shown as a green (carbon) calotte model (Schirle and MacRay, 2012, PDB ID 4OLB). Yellow part corresponds to the approximate size of Ago2 short isoforms. C) Surface charge displayed on the modelled structure of short Ago3-B. A portion of the RNA binding channel between the N and PAZ domain is preserved and retains positive charge (blue). It might interact with negatively charged RNA backbone phosphates via electrostatic interactions. Structure of full-length mouse Ago2 and short Ago3-B was predicted on the Phyre-2 server (Kelley & Sternberg, 2009). Surface potential was calculated on the APBS server (Baker et al., 2001; Dolinsky et al., 2007) .Structures were processed and visualised in PyMol 1.3.

4.2 Structural modelling of short AGOs

We next checked which Argonaute domains are encoded by mouse short transcripts. All short Argonaute protein isoforms (AGOs) span the N-terminal domain, while only AGO3 short isoforms stretch further into the N-portion of the PAZ domain. However, all isoforms terminate before the pocket binding the 3'-end of the guide RNA - Figure 11B. Structural modelling suggests that the major part of short AGOs adopts globular conformation with the exception of the highly unstructured N-terminus. The first 20 amino acids are absent in all available mammalian crystal structures, because this region is disordered and prevents crystallization. We speculated that the N-terminus extended on the surface of the PIWI domain could compete with the binding of tryptophan residues (green calotte model in Figure 11B) on the surface of the GW182/TNRC6 family proteins or some other AGO interacting partners. Altered N-terminus in maternal isoforms of the mouse AGO2 (MRDKLNF vs MYSGAGPV) is positively charged in the context of oocyte cytoplasm, while somatic N-terminus is neutral in physiological pH; whether this can have any impact on RNAi or miRNA pathways in oocytes remains to be tested.

Short AGO3 isoforms may non-specifically bind RNA backbone as a part of the positively charged N-PAZ channel is preserved - Figure 11C. Two negatively charged pockets on the surface of AGO3-B N-terminal domain may provide binding sites for interacting partners having positively charged surface residues Figure 11C.

4.3 Experimental validation

Based on our bioinformatics analysis, we decided to clone predicted isoforms from mouse oocytes for further experimentation. A cDNA library was prepared from ~100 fully grown (GV) oocytes collected from three superovulated C57Bl/6xCD1 females. RNA for the reverse transcription was extracted also from thymus, spleen and pancreas. Short *Ago* transcripts were amplified in the PCR reaction with isoform specific primers (see Material and Methods), gel-purified, and ligated into the pJET1.2 cloning plasmid (Fermentas). Potentially positive bacterial colonies were pre-screened with colony PCR and then cultured in the liquid media over night for the plasmid isolation. Sequencing of purified clones confirmed the presence of all predicted short *Ago* transcripts in oocytes. Moreover, the presence of *Ago3-A* and *Ago3-B* short transcripts was confirmed by in thymus and *Ago3-B* was also detected in spleen. These results suggested that especially *Ago3* short isoforms could have a physiologically relevant role in immune organs. Surprisingly, we observed common exon-skipping in *Ago3* short transcripts resulting, in some cases, in the premature translational termination because of frameshift mutations. We did not carried out any further analysis of these very short and likely aberrant transcripts.

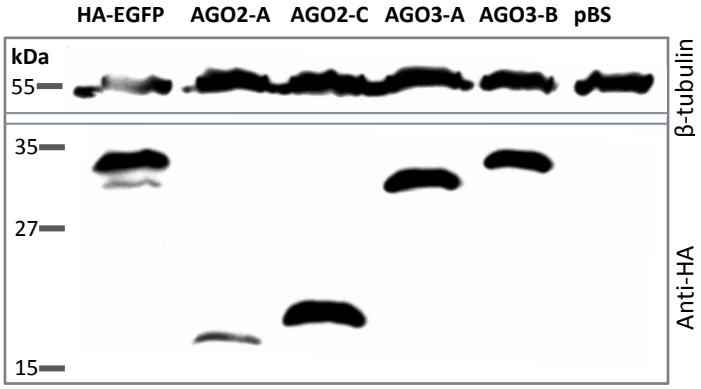

Figure 12 – Overexpression of short AGOs in cells
Western-blot analysis of HA-tagged short AGOs shows strong overexpression in mouse embryonic fibroblasts NIH3T3 after 48h in the culture except of AGO2-A. HA-EGFP is a positive control for anti-HA primary antibody staining (rat anti-HA IgG_1, Roche, 1:2500) and transfection efficiency. β-tubulin serves as a loading control. 40 µg/well of total protein lysate loaded on 12.5% SDS-PAGE gel. Film was developed for 10s with west-pico chemiluminiscent substrate.
See Material and Methods for more details.

Positive clones were amplified with ORF-specific primers containing restriction (AgeI and NotI) sites and ligated into pSV40 expression plasmid with a C-terminal HA tag. This vector was constructed from the original pSV40-HA plasmid (see Materials and Methods). We decided for the C-terminal tagging, because in this way the tag would not interfere with a possible function of the flexible Argonaute's N-terminus. HA-tagging

allowed for the immunostaining of western blot membranes and can be used in future experiments (i.e. for immunolocalization or immunopurification).

However, overexpression of only *Ago3* short transcripts from the SV40 (simian virus) promoter yielded detectable protein levels in both mouse NIH3T3 and human HeLa cells (data not shown). We therefore re-cloned HA-tagged coding sequences into the pCI/neo (Promega) expression plasmid which contains both cytomegalovirus enhancer and promoter usually providing high protein yields in transfected cells. Indeed, we obtained sufficient overexpression from the pCI/neo plasmids for all four Ago isoforms tested - Figure 12. The shortest *Ago2-A* was expressed at lower levels compared to others probably because of worse protein stability. Protein expression peaked after 24h and was still high after 48 hours (data not shown).

4.4 Probing impact of short Agos on the miRNA pathway

Despite obvious differences between somatic cells and oocytes, a possible impact of short AGOs on the miRNA pathway should be measurable in cultured cells with highly overexpressed isoforms and in combination with a sensitive reporter system.

4.4.1 Luciferase reporter system

We used well established luciferase reporter systems monitoring miR-30 or Let-7 miRNA activities (Ma et al. 2010). These systems consist of three reporter plasmids containing the luciferase coding sequence from marine coral *Renilla reniformis* (*Renilla* luciferase - RL) with different miRNA-binding sites added in the 3' UTR - Figure 13.

"Perfect" reporters contain a single entirely complementary target site for endogenous let-7a or miR-30c miRNAs, respectively Figure 13. Perfect reporters are predominantly suppressed by AGO2-mediated cleavage and thus reflect RNAi-like activity. "Bulged" reporters contain three mismatched nucleotides in the middle of miR-30 or let-7 target sites. The Let-7 reporter contains three bulged sites in a row, while the miR-30 reporter contains four. Bulged reporters reflect the activity of the miRNA pathway in translational inhibition and miRNA-induced RNA decay. Reporters with three and four bulged target-sites were chosen with a regard to the relative abundances of let-7 and miR-30 miRNAs in mouse oocytes.

Lastly, "Mutated" reporter plasmids contain three or four Let-7 or miR-30 target sites, respectively, with mutations in both seed and supplementary regions. Thus, mutated reporters serve as a non-targeted control. These three reporters are individually co-transfected with a tested protein and a control plasmid expressing firefly luciferase (pGL4 - Promega) in triplicates on the 24 well-plates. Cells are harvested after a defined time and luminescence in the cell lysate is measured first with the firefly luciferase substrate followed by the *Renilla* substrate which quenches the previous reaction.

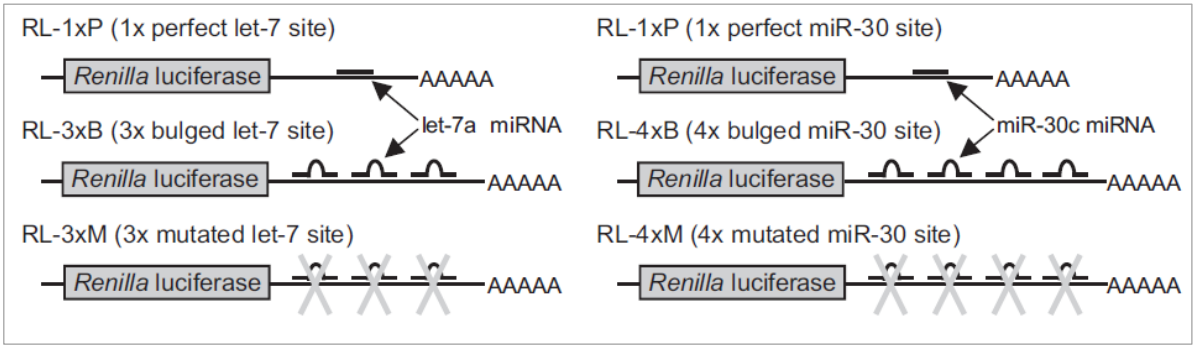

Figure 13 – Let-7 and miR-30 reporters monitoring RNAi-like and miRNA pathways
While perfect *Renilla* luciferase reporters are predominantly suppressed by AGO2-mediated mRNA cleavage (called RNAi-like mode/pathway), bulged reporters reflect the activity of the miRNA pathway (translational repression, deadenylation and RNA decay) employing respective endogenous miRNAs (Let-7 or miR-30 family). Mutated reporter serves as non-targeted control. Adopted from Ma et al., 2010

4.4.2 Calibration of the reporter system

Our hypothesis assumed that short AGOs would reduce the efficiency of the miRNA-mediated RNA silencing; therefore we expected to observe an increase in the luciferase signal for bulged reporters in samples transfected with AGOs compared to unrelated protein control (EGFP or LacZ). We sought to achieve the maximal reporter repression in order to see a possible rise in the signal caused by co-transfected proteins more clearly.

The miRNA intracellular pool as well as the abundance of RISC factors is, indeed, limited and the efficiency of the repression is therefore influenced mainly by the concentration of miRNA target sites. We therefore calibrated the reporter system by decreasing amounts of the RL reporter while keeping the concentration of non-targeted firefly luciferase (FL) constant across all samples. The total amount of transfected DNA

was adjusted with pBluescript plasmid DNA ("stuffer") to 500 ng per well and luciferase activities were measured 48 hours post-transfection. Measured values were normalized to FL activity and the signal from mutated RL reporter was set to one for each tested concentration. Our measurements showed that target repression was inversely proportional to the amount of transfected plasmids for both let-7 and miR-30 reporters in mouse NIH3T3 cells -. It is likely that this reflects a correlation to the number of target RNA molecules produced from reporter plasmids. However, it is not possible to decrease the amount of transfected reporters significantly below approx. 1ng, because the luminometer readout for perfect and bulged reporters gets too close to background values. We found that the transfection of 2 ng for miR-30 reporters and 5 ng for the Let-7 reporters in combination with 25 ng of the control FL luciferase per well ensures sufficient repression combined with a reliable luminescence readout.

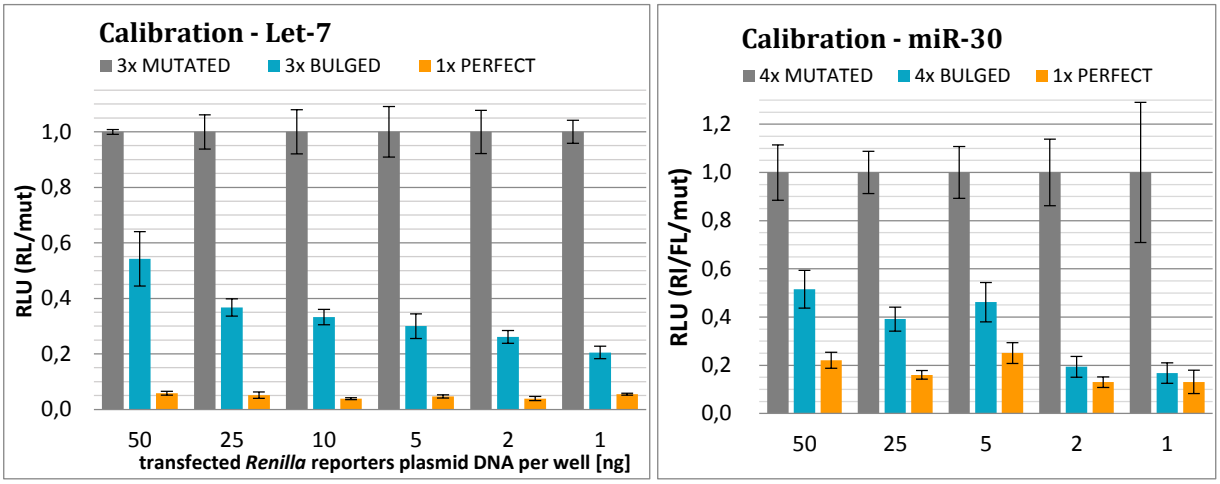

Figure 14 – Calibration of *Renilla* luciferase reporter systems
This two plots show that the miRNA-mediated repression of "bulged" *Renilla* luciferase reporters having three let-7 or four miR-30 target sites in 3' UTR of respective mRNAs is concentration dependent. The miRNA pathway represses more efficiently the lower amounts of reporter mRNAs (data were normalized to the non-targeted "mutated" control). Cellular miRNA machinery is saturated with the high reporter concentrations resulting in the ineffective miRNA-mediated repression. Perfectly complementary targets are silenced more quickly and concentration effect is not apparent after 48h hours post-transfection. Experiments were repeated three times in triplicates. The RLU on the vertical axis stands for "relative luciferase unit". Raw luminescence values were normalized to the co-transfected firefly luciferase (for miR-30 reporters) and the signal for mutated RL was set as one for each concentration tested. Error bars indicates ± standard deviation (SD) from three experiments (the same apply for error bars in the rest of this thesis). See Material and Methods for experimental details.

4.4.3 No impact of short AGOs on the miRNA pathway

To test our hypothesis we then co-transfected pCI/neo expression plasmids encoding either short AGOs or the control proteins (EGFP – enhanced green fluorescent protein, or β-lactamase – LacZ) with individual RL reporters to mammalian cells. Reporter concentrations used were the same as indicated in the previous section. After promising initial measurements, which used only the red fluorescent protein and GFP as controls (not shown), the addition of more controls (LacZ and pBluescript, which does not encode any protein product) revealed that even the overexpression of miRNA-unrelated proteins can influence the repression efficiency in the range of ~20% (clearly visible in the fig. 16 - left panel). This fact underscores the importance of reliable controls for valid interpretation of data from luciferase reporter experiments.

Although *Ago3-B* isoform seemed to have some mild influence on the repression of let-7 reporters compared to control proteins – fig. 16, this effect completely disappeared when miR-30 reporters were used – fig. 15. We conclude that short AGOs have no impact on the reporter system when ectopically expressed in mouse NIH3T3 cells or in human HeLa cells. However, involvement of short AGOs in other biological processes not addressed by our experimental design is still possible.

Despite the falsification of our hypothesis, measured data contain additional valuable information. Clearly, the activity of each reporter system is cell-type dependent, likely reflecting different levels of endogenous miRNAs (compare repression of targeted bulged and perfect *Renilla* reporters between cell lines fig. 15 and 16).

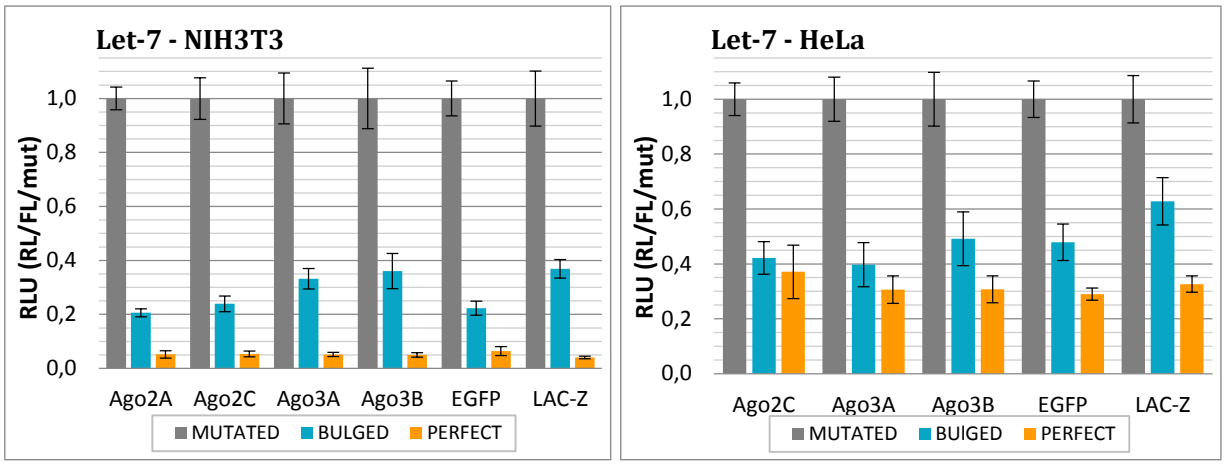

Figure 16 – Functional test of short AGOs using the Let-7 *Renilla* luciferase reporter system
Short Argonaute protein isoforms have no impact on the behavior of the let-7 luciferase reporter system neither in mouse NIH3T3 cells (left panel) nor in human HeLa cells (right panel). Results show relatively high variability for "bulged" *Renilla* reporter in used controls (EGFP and LacZ) especially in NIH 3T3 cells. Note overall difference in the reporter repression between 3T3 and HeLa cells likely caused by the different abundance of endogenous miRNAs of respective families. Data from three independent experiments performed in triplicates are shown. 5ng of each individual reporter was co-transfected with 25 ng of FL and 470 ng of each expression plasmid tested. Cells were cultured for ~48 hours.

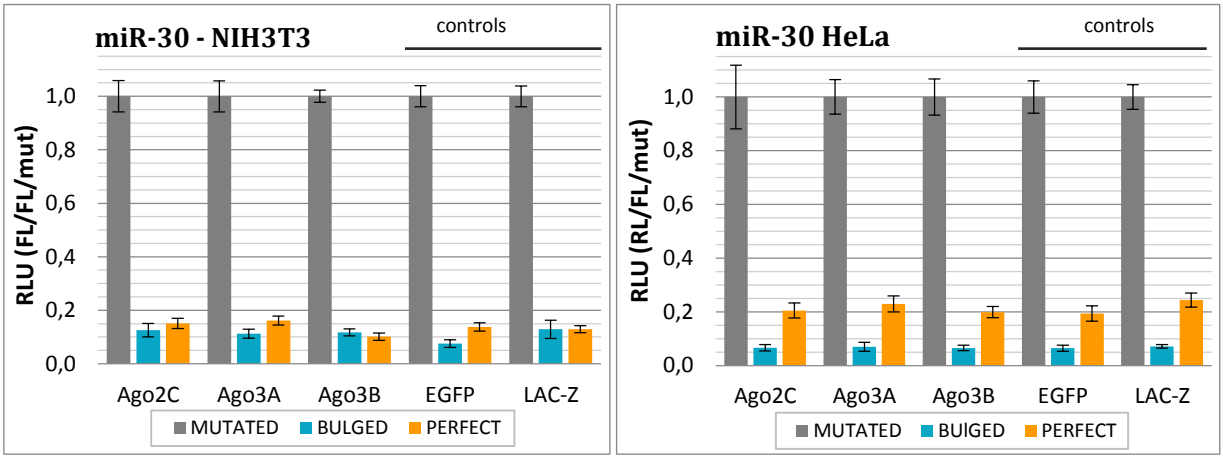

Figure 15 – Functional test of short AGOs using miR-30 *Renilla* luciferase reporter system
Similar experiment to those shown in the Graph above were performed with miR-30 *Renilla* luciferase reporter system with the exception that only 2 ng of each RL reporter were used. This data confirms that short AGOs do not simply influence the miRNA pathway in cultured mammalian cells. Experiment was repeated two and three times in triplicates for NIH3T3 and HeLa cells, respectively.

4.4.4 Additional control experiments

First, in order to exclude a possibility that our results were biased by the low *Renilla* reporter concentration, we repeated experiments with 50 ng of miR-30 *Renilla* reporters in NIH3T3 cells including additional control pBluescript (pBS) plasmid, which is not encoding for any protein that would be expressed in mammalian cells. Results confirmed our previous data, ruled out a possible concentration dependent effect of short AGOs on the miRNA pathway, and again pointed out to non-specific effects induced by the ectopically expressed EGFP – fig. 17. However the data nicely fit the calibration measurements confirming that the stoichiometry between miRNAs and its targets, indeed, matters (compare with fig. 14)

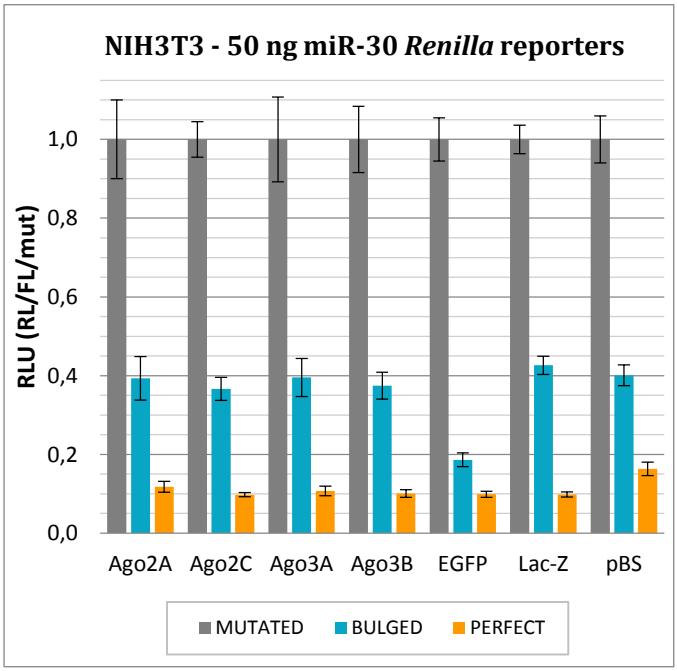

Figure 17 – An effect of short AGOs is concentration independent
This experiment differed from previous two only by the higher amount of *Renilla* reporter plasmids transfected into the cells. Correspondingly, amount of transfected expression plasmids was decreased slightly to 425 ng. This should not have any impact on the result. This plot clearly demonstrates that short AGOs do not influence miRNA pathway either in the presence of 25x higher target concentration when compared to control proteins. Three independent experiments in triplicated were performed.

To verify that our reporter system specifically respond to the miRNA pathway and to the defined changes within it, we first tried to knockdown *Ago2* and *Dicer1* using a short hairpin RNA (shRNA) expressing plasmids. We observed de-repression of RL reporters in samples treated with shRNA plasmids compared to the pBS, EGFP or LacZ controls. However, observed target de-repression was not caused by the specific down-regulation of DICER or AGO2 proteins, because the same effect was induced by the shPKR plasmid (targeting protein kinase R that is unrelated to miRNA pathway) suggesting a non-specific effect probably stemming from the saturation of miRNA biogenesis machinery by short hairpin substrates. This might have impeded the

biogenesis of endogenous miRNAs including miR-30 miRNA family. Alternatively, the number of shRNA-derived miRNAs outcompeted endogenous miRNAs in the RISC-binding. In any case, it was likely a change in the stoichiometry of endo- and exogenous miRNAs resulting in the observed reporter de-repression rather than a change on the protein level. We did not checked knockdown efficiency on the protein level, but as far as targeted RL reporters were still moderately repressed, we assume that DICER and especially AGO2 proteins must have still been present also in the cells transfected with *Dcr1* or *Ago2* shRNA plasmids.

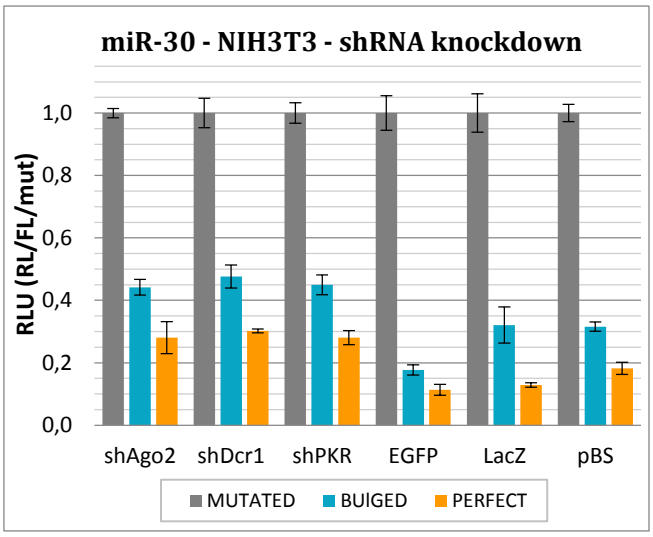

Figure 18 – *Ago2* and *Dicer1* knock-down
These results show that shRNA expression plasmids rather generally alter small RNA pathways in cells than induce specific downregulation of respective proteins. 25ng of RL and FL luciferase reporter plasmids and 450 ng of shRNA or control plasmids was used for transfection. Shown are averaged data from two biological replicates.

Because of unconvincing knock-down results, we used antagomirs; chemically-modified target mimics, which cannot be cleaved by AGO2. Antagomirs tightly bind complementary miRNAs loaded on Argonaute proteins and in this way prevent miRISCs from the recognition of their targets. We tested the impact of let-7 family antagomirs and miR-30c antagomirs on miR-30 and Let-7 RL reporters. Luminescence was measured two days post-transfection. Transfection of the heterogeneous combination of plasmids and small RNA analogs required the use of Lipofectamine 2000 reagent (Thermo Scientific). We observed specific and highly efficient de-repression of Let-7 RL reporters treated with anti-Let-7 antagomirs (Exiqon) for both miRNA and RNAi-like silencing modes.

Interestingly, the signal coming from de-repressed targeted reporters appeared even higher than the signal from the mutated control. This could either reflect slight difference in RNA stability or in translation rates of the mutated reporter. Alternatively, changed sequence of Let-7 target sites in the mutated reporter might provide novel

target-sites for other endogenous miRNAs. We don't know the exact reason; moreover displayed data come just from a single experiment. In any case, anti-Let-7 antagomirs induced highly effective and specific de-repression of Let-7 target reporters and did not influence the miR-30 RL reporter system.

miR-30 antagomir (Exiqon), which we have used, selectively inhibits only a single miR-30 family member miR-30c, therefore only the perfect miR-30 reporter containing a single exact miR-30c target site is fully de-repressed, while the 4x bulged reporter is still down-regulated, presumably, by the other miR-30 family members in the cells.

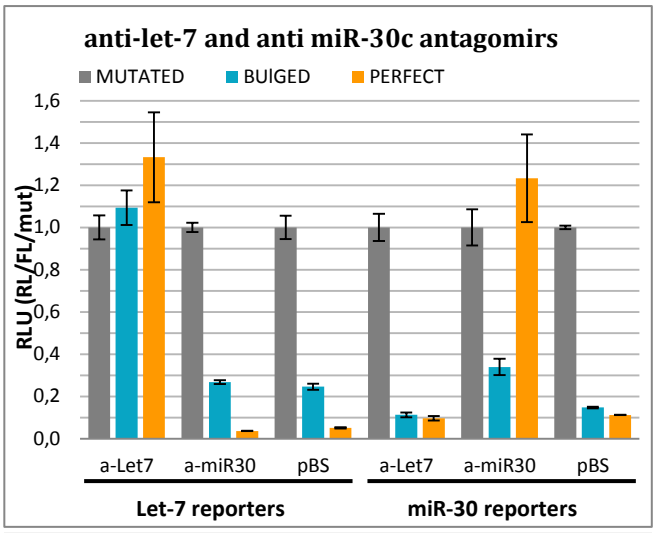

Figure 19 – Anti let-7 and miR-30 antagomirs
This graph clearly shows that the mix of anti-Let7 family antagomirs specifically and efficiently blocks the repression of let-7 reporters and confirms the sensitivity of Let-7 RL reporter system to specific changes in the miRNA pathway. Anti-miR-30c antagomirs cause complete de-repression of the perfect reporter but perform worse for the bulged reporter because it is still repressed by the other members of miR-30 family. Data from a single experiment are shown. See Material and Methods for experimental details.

We conclude that the reporter system we used in this work responds to the relative changes in the abundance of miRNAs and can be used for a probing miRNA activity in cultured cells. However, proper controls are essential to avoid false positive results. The behaviour of these reporter systems should be tested and optimized for each cell type prior to the serious experiments. Our data suggest, that miRNA regulation is rather complex and that the output from the seemingly simple reporter system is influenced by many factors.

4.5 Generation of *Ago2* deficient cell line

To have a control lacking AGO2 for luciferase reporter experiments, we decided to generate *Ago2*-deficient NIH3T3 cell line. To this end, we used CRISPR/Cas9 genome editing technology, which was recently introduced for the generation of many transgenic model organisms and cell-lines (Doudna & Charpentier 2014). The spCas9 from bacterium *Streptococcus pyogenes* is a DNA endonuclease programmable by short guide RNAs (sgRNAs), which contain 18-nt long variable region on their 3'end. This short RNA sequence is used by the Cas9 nuclease for specific recognition of complementary target sequences in DNA. The Cas9 introduces double-stranded DNA breaks in complementary loci, which are then sealed by cellular DNA damage repair pathways. It can be either repaired by the homologous recombination if some complementary template (endogenous or experimentally provided) is available or by the error-prone non-homologous end joining (NHEJ) pathway. NHEJ often generates short insertions and deletions resulting in frameshift mutations (Doudna & Charpentier 2014).

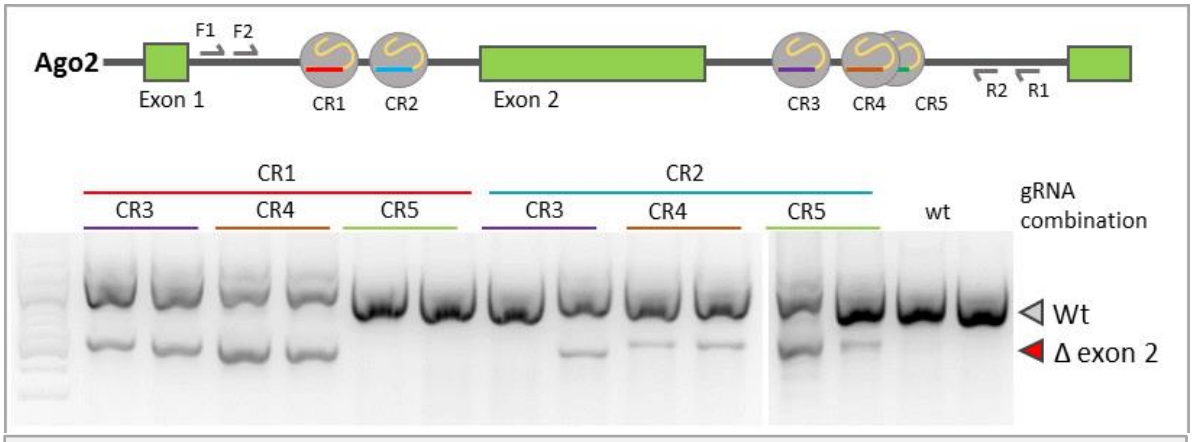

Figure 20 – Design of sgRNAs for elimination of exon-2 of the mouse *Ago2*
Top scheme shows the positions of designed sgRNAs guiding spCas9 (gray circles) nuclease to for cleavage in introns flanking the exon-2 of the *Ago2* gene. Agarose gel bellow the scheme displays the performance of different sgRNA combinations in the excision of the exon2. Shorter~~500bp long band indicates successful deletion. DNA was isolated from NIH3T3 cells two days post-transfection and used in the nested PCR reaction with F1/R1 primers in the first round and F2/R2 primers in the second round (each round 25 cycles, 40s extension time, Taq polymerase – Thermo Scientific). Marker in the first line is the 100bp Gene Ruler (Thermo Scientific). 250 ng of each pU6-sgRNA plasmid expressing designed sgRNA from the U6 promoter was used.

We designed five sg RNAs with target sites in introns adjacent to the exon-2 of the *Ago2* gene. Synthetic DNA oligonucleotides were annealed and ligated into pU6-sgRNA backbone plasmid (made in house) which expresses sgRNA under the U6 promoter. Individual plasmid clones with speicific sgRNAs called CR1-CR5 were amplified in bacterial cells and purified plasmids were sequenced for verification.

We used a pair of sgRNAs to excise the entire exon-2 assuming that resected DNA will be repaired by NHEJ, while the excised ~500-bp DNA fragment will be degraded. The loss of the exon 2 should result in the frameshift mutation in spliced *Ago2* transcripts leading to the premature termination of translation. The NIH3T3 cell-line stably expressing Cas9 established in our laboratory (work of R. Malik, unpublished) simplified the initial testing of sgRNA pairs. Cells were transfected with the different pairs of pU6-sgRNA plasmids and genomic DNA was isolated two days later. To assess the editing efficiency we used PCR reaction producing ~1-kbp wild-type and ~500-bp long mutated product indicating exon-2 loss. First experiments with combinations of different sgRNAs (250 ng each plasmid) allowed us to identify active sgRNA combinations (Figure 20). Next, we tested the impact of sgRNA plasmid concentration on deletion efficiency (Figure 21). Transfection of 100 ng of each pU6-sgRNA plasmid supplemented with 500ng of pBS stuffer plasmid DNA yielded the highest deletion rates. Surprisingly higher amounts of transfected pU6-sgRNA plasmids resulted in worse editing performance.

	Deletion efficiency			
sgRNA	1+3	1+4	2+3	2+4
100 ng	26%	62%	39%	18%
250 ng	12%	60%	25%	13%
350 ng	12%	50%	20%	9%

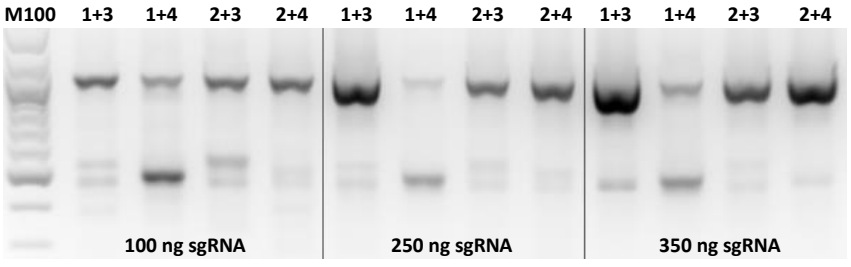

Figure 21 – Impact of the pU6-sgRNA plasmid amount on deletion efficiency
This figure shows that lower amounts (100 ng each) of transfected sgRNA expressing plasmids result in superior deletion rates. sgRNA pair CR1+4 identified in the previous experiment was confirmed as the best performing combination. The amount of transfected DNA was adjusted with pBS stuffer plasmid to 700ng. Table displays deletion efficiency calculated as a signal intensity of the mutated bands (shorter) on the agarose gel compared to the total DNA signal in respective lines. Signal was measured in ImageJ. Simple PCR with primers F2/R2 was carried out and loaded on 1.5% agarose gel. M100 -100bp Gene Ruler – DNA Ladder (Thermo Scientific/Fermentas)

The best performing sgRNA pair "CR1+CR4" was then used to generate *Ago2*-deficient cell-lines from the initial NIH3T3-spCas9 cell line (clone #E8). Cells were re-plated 24h post-transfection in the low density on 15 cm petri dishes to generate clonal colonies originating from single cells. DNA was isolated from expanded clonal populations approx. one month later and the touchdown PCR was used for the identification of mutated clones. Positive hits were verified by the sequencing. We detected four positive clones out of 32 tested; subsequent analysis revealed that all four were heterozygous.

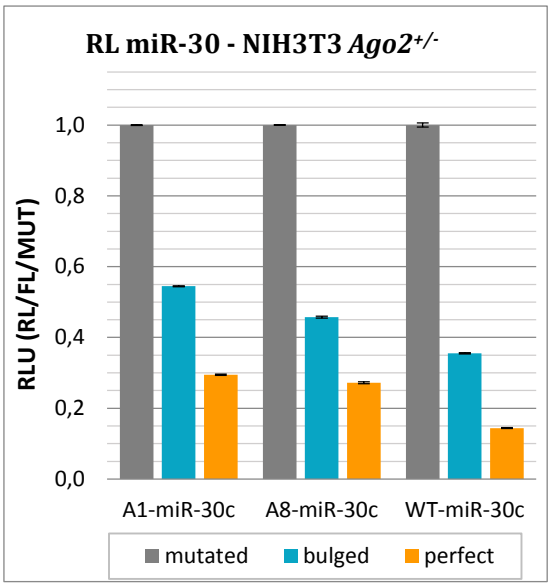

Figure 22 – miRNA activity in *Ago2*$^{+/-}$ NIH3T3 cells
miRNA activity of heterozygous *Ago2*$^{+/-}$ clones #A1 and #A8 was tested with miR-30 RL reporters. The loss of single *Ago2* allele resulted in slight de-repression of both bulged and perfect RL reporters compared to wild-type control. 25ng of RL and 25 ng of FL plasmids supplemented with pBS to 500ng was transfected. Only the single experiment was performed.

We tested two of our heterozygous *Ago2*$^{+/-}$ cell lines #A1 and #A8 in the dual luciferase assay described in the previous chapter. We observed marked de-repression of both bulged and perfect miR-30 RL reporters suggesting that even a loss of single *Ago2* allele compromises miRNA activity – fig. 22. Effect is more pronounced for the perfect miR-30 reporter containing only the single miR-30c target site which is more sensitive to the loss of the AGO2 slicer activity.

These cell clones will be used in the near future for the second round of the mutagenesis to generate cell lines completely lacking *Ago2.* Such cell lines can be used for the studies of *Ago2* cellular functions and will serve as a useful control not only in luciferase reporter experiments. Even better control cell line with catalytically inactive AGO2 can be made in the future with CRISPR/Cas9 technology.

5 Discussion

In this thesis, I described the discovery of novel short *Ago2* and *Ago3* transcripts in mouse oocytes. We were able to verify their presence in oocytes, spleen and thymus. Functional analysis employing *Renilla* luciferase system however suggested, that short AGO protein do not influence miRNA or RNAi-like small RNA pathways.

Our measurements of the luciferase reporter activity in different cellular contexts or at a variable reporter concentration reflected inherent properties of cell lines used. An abundance of certain miRNA classes apparently influence extent of *Renilla* reporter repression. The most pronounced difference was observed between mouse NIH3T3 cells and human HeLa cells with let-7 *Renilla* reporters. While miRNA pathway represses reporters efficiently in NIH3T3 cells, luciferase activity remains relatively high in HeLa cells, which likely produce less let-7 miRNAs (Ma et al. 2010). In contrast, miR-30 *Renilla* reporters are repressed more effectively and differences between mouse and human cell lines are less marked. This suggests that independent reporter systems should be used in parallel to avoid incorrect interpretation of data.

A similar situation applies also for experimental controls. In figures 17 and 18, EGFP seems to influence reporter activity quite markedly. However, it was previously reported that this is non-specific effect linked to the cytotoxicity of EGFP caused in part by the production of dsRNA from the EGFP-ORF inducing the PKR-dependent interferon response (Nejepinska et al. 2014). Not only raw luminescence values are markedly lover for cells expressing ectopic EGFP, but also high (EGFP) siRNA titers may saturate endogenous RISC and thus shift results (Nejepinska et al. 2014). However, the decrease in luminescence in EGFP samples should be rather attributed to the limited transcription of reporter plasmids caused by PKR and thus to the concentration-dependent effect of miRNA targets as seen in the calibration of reporters in fig. 14.

Several additional layers of complexity complicate prediction of miRNA binding and function, as well as outcomes of experiments with reporter plasmids. Among still poorly understood factors is competition of RISC with other RNA binding proteins, an influence of a secondary structures in targeted RNAs on the RISC binding, and a contribution of binding partners associated with different mammalian Argonautes (discussed in Ameres & Zamore 2013, Bartel 2009). Moreover, relative concentration of small RNAs, of

individual Argonaute paralogs, of downstream enzymes and scaffold proteins, and the crosstalk with other RNA metabolic pathways, all influence output of the RNA silencing and make the problem extremely complex and context dependent.

HTS data from mouse oocytes suggest that also transcription of the full-length *Ago2* starts on the alternative maternal exon. Catalytic activity of AGO2 is essential for active RNAi in mouse oocytes (Stein et al. 2015). It is possible that altered N-terminus in maternal AGO2 has some impact on activity or stability of the protein. Thus, it would be interesting to compare an influence of the maternal full-length AGO2 isoform with standard somatic AGO2 variant with luciferase reporters in similar experiments as were performed here. The *Ago2*-deficient cell line will be absolutely essential for this experiment having no background AGO2 activity. Overall, only two and three peptides originating from AGO2 and AGO3, respectively, were detected in recent deep-proteomic data, which were able to identify approx. 5000 different proteins in oocytes (Pfeiffer et al. 2015). This suggests that even a small number of full-length AGO2s in oocytes is able to support active RNAi.

It is worth mentioning that no interacting partners of the N-terminal domain have been reported yet. As the N-terminal domain has likely regulatory roles in the cleavage of passenger and target strands (Faehnle et al. 2013, Hauptmann et al. 2013, Nakanishi et al. 2013), it will be important to identify such interacting partners or/and possible post-translational modifications. Our short expression constructs might be used for the proteomic study which could answer these questions.

The short proline-rich stretch in the very N-terminal end of both AGO2 and AGO3 was suggested to masks binding surface on the PIWI domain used for the interaction with Dicer (Wilson & Doudna 2013), it is therefore likely that N-terminal domain is post-translationaly modified as a part of RISC maturation and again different N-terminus in the maternal AGO2 might interact with the PIWI domain in a different way possibly resulting in a changed accessibility of the PIWI surface for the binding of Dicer or other factors. Interestingly, a rendering of the electrostatic surface potential for mouse AGO2 revealed two negatively charged pockets in the N-terminal domain which might provide binding sites for interacting partners (Figure 11).

What turns miRNA pathway inactive in mouse oocytes remains elusive. Our study ruled out one of potential factors inhibiting miRNA pathway in oocytes, while leaving RNAi unaffected. I suggest that the miRNA inactivity in oocytes is rather multifactorial phenomenon.

First of all, concentrations of all factors involved in the miRNA biogenesis and miRNA-mediated repression must be taken into account. Both global proteomic and deep-sequencing data suggest that some critical components of the miRNA pathway are either missing or present in very low amounts in fully grown GV oocytes. Among them AGO1, AGO4, TNRC6a and EDC3 are practically missing. As EDC3 bridges CCR4:NOT complex with the decapping machinery; decapping seems to be uncoupled from the deadenylation in oocytes. Furthermore Dcp1a and Dcp2 are dormant maternal mRNAs, which enter translation later in MII eggs and contribute to the clearance of maternal transcripts in zygotes (Ma et al. 2013). This notion is supported by the observation, that deadenylated mRNAs are generaly not degraded in oocytes. This regulatory scheme apparently applies for hundreds of dormant transcripts, which are not detected in the proteome despite being abundantly represented in the oocyte transcriptome (Pfeiffer et al. 2015, Wang et al. 2010).

Second, miRNAs are approximately in 1:7 ratio with endo-siRNAs. These small RNAs compete for the binding in a limited pool of Argonautes. While siRNAs occupy majority of available Argonautes and induce AGO2-mediated cleavage of perfect targets, a dynamics of the miRNA regulation is probably limited by the lack of TNRC6/GW182 cofactors and by the uncoupling of the decapping machinery from CCR4:NOT deadenylation complex. Furthermore, a tremendous number of potential target sites in gradually accumulating transcripts turns miRNA regulation ineffective as the chance of encountering cognate target by miRISC decreases.

It would be therefore interesting to study to what extent the deadenylation of miRNA targets really work in oocytes and how is the translation inflicted. However research of the miRNA pathway in oocytes seems to be partly resolved by the fact that Dgcr8-/- oocytes lacking canonical miRNAs can develop into the blastocyst. Research in mammalian oocytes is hampered by the limited source of experimental material. Both proteome and transcriptome in oocytes significantly differ even from ES cells, thus

oocytes cannot be easily replaced by any model cell-line, which would allow for classical high-throughput biochemical analysis.

Here we showed that short Argonaute isoforms do not impact miRNA pathway capacity to repress ectopically expressed reporters in mammalian cells. However we cannot rule out the functional importance of short AGOs in the native context of mouse oocytes or their other possible functions which we did not addressed in our research design. Future experiments regarding short Agos should investigate their subcellular localization both in transfected cells and in fixed oocytes.

6 Supplementary information

6.1 Sequences of short Argonaute proteins

AGO2A

MRDKLNFLASPAPTTSPIPGYAFKPPPRPDFGTTGRTIKLQANFFEMDIPKIDIYHYELDIKPEKCPRRVNREI
VEHMVQHFKTQIFGDRKPVFDGRKNLYTAMPLPIGRDKEIASPGRHGRLPCVGFFMRAR*

AGO2C

MRDKLNFLASPAPTTSPIPGYAFKPPPRPDFGTTGRTIKLQANFFEMDIPKIDIYHYELDIKPEKCPRRVNREI
VEHMVQHFKTQIFGDRKPVFDGRKNLYTAMPLPIGRDKEIRGSLKARARRKRKSQSKSRSMN*

AGO3A

MEIGSAGPIGAQPLFIVPRRPGYGTMGKPIKLLANCFQVEIPKIDVYLYEVDIKPDKCPRRVNREVVDSMVQH
FKVTIFGDRRPVYDGKRSLYTANPLPVATTGVDLDVTLPGEGGKDRPFKVSVKFVSRVSWHLLHEALAGGT
LPEPLELDKPVSTNPVHAVDVVLRHLPSMKYTPVGRSFFSAPEGYDHPLGGGREVWFGFHQSVRPAMWKM
MLNIDDCYSISSSLVSPS*

AGO3B

MEIGSAGPIGAQPLFIVPRRPGYGTMGKPIKLLANCFQVEIPKIDVYLYEVDIKPDKCPRRVNREVVDSMVQH
FKVTIFGDRRPVYDGKRSLYTANPLPVATTGVDLDVTLPGEGGKDRPFKVSVKFVSRVSWHLLHEALAGGT
LPEPLELDKPVSTNPVHAVDVVLRHLPSMKYTPVGRSFFSAPEGYDHPLGGGREVWFGFHQSVRPAMWKM
MLNIDVSATAFYKAQPVIQFMCEVLDIHNIDEQPRPLTDSHRVKFTKEIKDNFQLVV*

6.1.1 miRNA sequences used in miR-30 *Renilla* reporters

A) Alignment of mouse miR-30 family miRNAs. B) Sequences of perfect, bulged and mutated target sites in miR-30 *Renilla* luciferase reporter plasmids (Adopted from Ma et al. 2013)

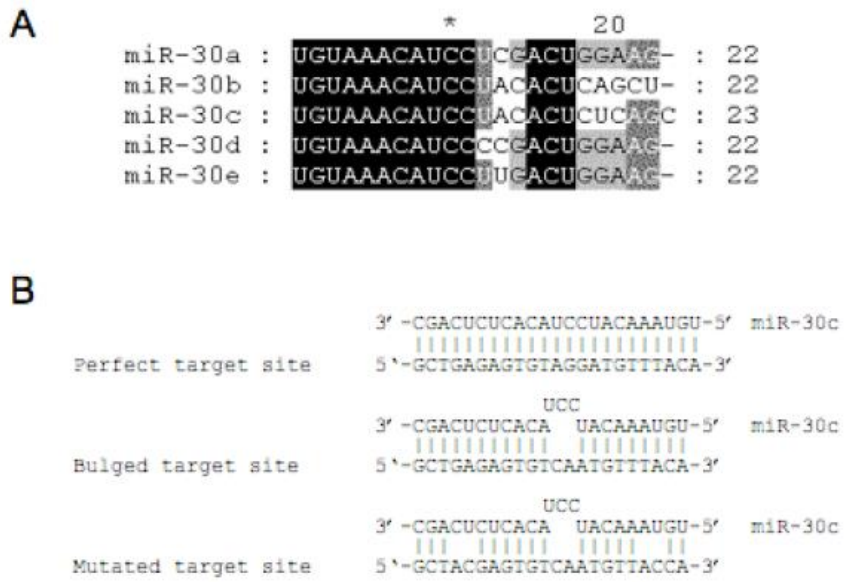

6.2 Plasmid maps

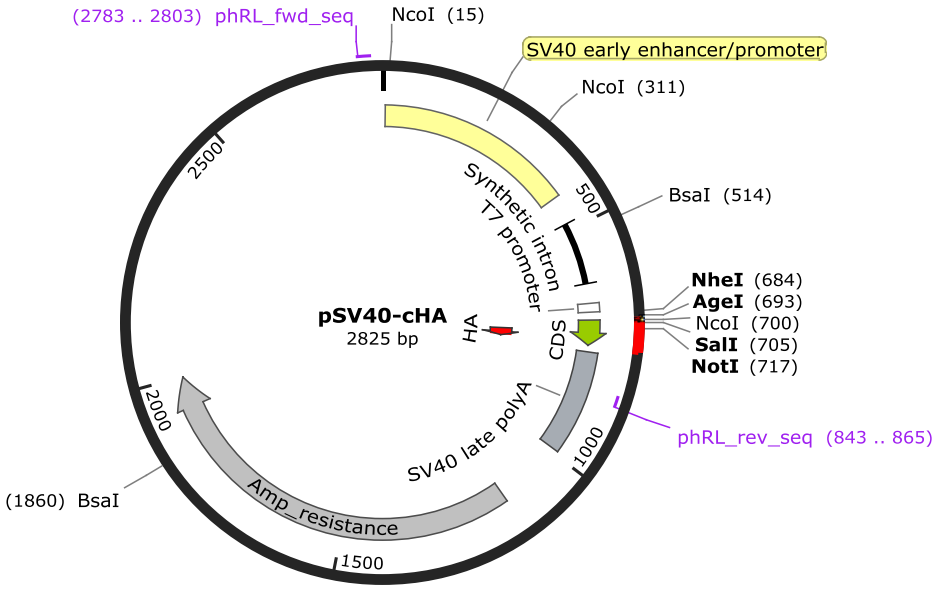

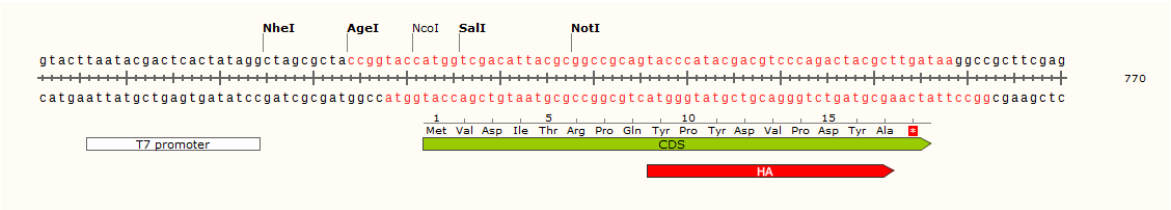

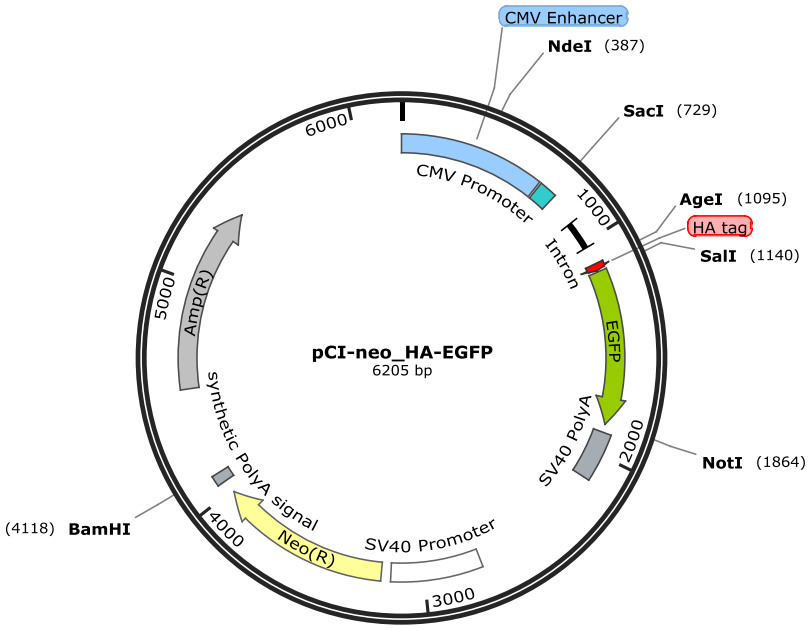

7 References

Abe K, Yamamoto R, Franke V, Cao M, Suzuki Y, et al. 2015. The first murine zygotic transcription is promiscuous and uncoupled from splicing and 3′ processing. *The EMBO Journal*. e201490648

Ameres SL, Zamore PD. 2013. Diversifying microRNA sequence and function. *Nature Reviews Molecular Cell Biology*. 14(8):475–88

Aravin A, Gaidatzis D, Pfeffer S, Lagos-Quintana M, Landgraf P, et al. 2006. A novel class of small RNAs bind to MILI protein in mouse testes. *Nature*. 442(7099):203–7

Babiarz JE, Ruby JG, Wang Y, Bartel DP, Blelloch R. 2008. Mouse ES cells express endogenous shRNAs, siRNAs, and other Microprocessor-independent, Dicer-dependent small RNAs. *Genes Dev.* 22(20):2773–85

Baek D, Villén J, Chanseok Shin, Camargo FD, Gygi SP, Bartel DP. 2008. The impact of microRNAs on protein output. *Nature*. 455(7209):64–71

Baker NA, Sept D, Joseph S, Holst MJ, McCammon JA. 2001. Electrostatics of nanosystems: Application to microtubules and the ribosome. *PNAS*. 98(18):10037–41

Bartel DP. 2009. MicroRNAs: Target Recognition and Regulatory Functions. *Cell*. 136(2):215–33

Behm-Ansmant I, Rehwinkel J, Doerks T, Stark A, Bork P, Izaurralde E. 2006. mRNA degradation by miRNAs and GW182 requires both CCR4:NOT deadenylase and DCP1:DCP2 decapping complexes. *Genes Dev.* 20(14):1885–98

Bernstein E, Caudy AA, Hammond SM, Hannon GJ. 2001. Role for a bidentate ribonuclease in the initiation step of RNA interference. *Nature*. 409(6818):363–66

Bernstein E, Kim SY, Carmell MA, Murchison EP, Alcorn H, et al. 2003. Dicer is essential for mouse development. *Nature Genetics*. 35(3):215–17

Billy E, Brondani V, Zhang H, Müller U, Filipowicz W. 2001. Specific interference with gene expression induced by long, double-stranded RNA in mouse embryonal teratocarcinoma cell lines. *PNAS*. 98(25):14428–33

Broderick JA, Zamore PD. 2014. Competitive Endogenous RNAs Cannot Alter MicroRNA Function In Vivo. *Molecular Cell*. 54(5):711–13

Burroughs AM, Ando Y, de Hoon ML, Tomaru Y, Suzuki H, et al. 2011. Deep-sequencing of human Argonaute-associated small RNAs provides insight into miRNA sorting and reveals Argonaute association with RNA fragments of diverse origin. *RNA Biology*. 8(1):158–77

Carmell MA, Girard A, van de Kant HJG, Bourc'his D, Bestor TH, et al. 2007. MIWI2 Is Essential for Spermatogenesis and Repression of Transposons in the Mouse Male Germline. *Developmental Cell*. 12(4):503–14

Carroll AP, Tooney PA, Cairns MJ. 2013. Context-specific microRNA function in developmental complexity. *Journal Of Molecular Cell Biology*. 5(2):73–84

Cecere G, Grishok A. 2014. A nuclear perspective on RNAi pathways in metazoans. *Biochimica et Biophysica Acta (BBA) - Gene Regulatory Mechanisms*. 1839(3):223–33

Cheloufi S, Dos Santos CO, Chong MMW, Hannon GJ. 2010. A dicer-independent miRNA biogenesis pathway that requires Ago catalysis. *Nature*. 465(7298):584–89

Chen Y, Boland A, Kuzuoğlu-Öztürk D, Bawankar P, Loh B, et al. 2014. A DDX6-CNOT1 Complex and W-Binding Pockets in CNOT9 Reveal Direct Links between miRNA Target Recognition and Silencing. *Molecular Cell*. 54(5):737–50

Christie M, Boland A, Huntzinger E, Weichenrieder O, Izaurralde E. 2013. Structure of the PAN3 Pseudokinase Reveals the Basis for Interactions with the PAN2 Deadenylase and the GW182 Proteins. *Molecular Cell*. 51(3):360–73

Claycomb JM. 2014. Ancient Endo-siRNA Pathways Reveal New Tricks. *Current Biology*. 24(15):R703–15

Cullen BR, Cherry S, tenOever BR. 2013. Is RNA Interference a Physiologically Relevant Innate Antiviral Immune Response in Mammals? *Cell Host & Microbe*. 14(4):374–78

Czech B, Hannon GJ. 2011. Small RNA sorting: matchmaking for Argonautes. *Nature Reviews Genetics*. 12(1):19–31

Decker CJ, Parker R. 2012. P-Bodies and Stress Granules: Possible Roles in the Control of Translation and mRNA Degradation. *Cold Spring Harbor Perspectives in Biology*. 4(9):a012286–a012286

Deerberg A, Willkomm S, Restle T. 2013. Minimal mechanistic model of siRNA-dependent target RNA slicing by recombinant human Argonaute 2 protein. *PNAS*. 110(44):17850–55

De Fazio S, Bartonicek N, Di Giacomo M, Abreu-Goodger C, Sankar A, et al. 2011. The endonuclease activity of Mili fuels piRNA amplification that silences LINE1 elements. *Nature*. 480(7376):259–U148

Deng W, Lin H. 2002. miwi, a Murine Homolog of piwi, Encodes a Cytoplasmic Protein Essential for Spermatogenesis. *Developmental Cell*. 2(6):819–30

Ding S-W, Voinnet O. 2007. Antiviral Immunity Directed by Small RNAs. *Cell*. 130(3):413–26

Dolinsky TJ, Czodrowski P, Li H, Nielsen JE, Jensen JH, et al. 2007. PDB2PQR: expanding and upgrading automated preparation of biomolecular structures for molecular simulations. *Nucl. Acids Res.* 35(suppl 2):W522–25

Doudna JA, Charpentier E. 2014. The new frontier of genome engineering with CRISPR-Cas9. *Science*. 346(6213):1258096–1258096

Elkayam E, Kuhn C-D, Tocilj A, Haase AD, Greene EM, et al. 2012. The Structure of Human Argonaute-2 in Complex with miR-20a. *Cell*. 150(1):100–110

Eulalio A, Huntzinger E, Izaurralde E. 2008. GW182 interaction with Argonaute is essential for miRNA-mediated translational repression and mRNA decay. *Nature Structural and Molecular Biology*. 15(4):346–53

Fabian MR, Sonenberg N. 2012. The mechanics of miRNA-mediated gene silencing: a look under the hood of miRISC. *Nature Structural & Molecular Biology*. 19(6):586–93

Faehnle CR, Elkayam E, Haase AD, Hannon GJ, Joshua-Tor L. 2013. The Making of a Slicer: Activation of Human Argonaute-1. *Cell Reports*. 3(6):1901–9

Fire A, Xu S, Montgomery MK, Kostas SA, Driver SE, Mello CC. 1998. Potent and specific genetic interference by double-stranded RNA in Caenorhabditis elegans. *Nature*. 391(6669):806

Flemr M, Malik R, Franke V, Nejepinska J, Sedlacek R, et al. 2013. A Retrotransposon-Driven Dicer Isoform Directs Endogenous Small Interfering RNA Production in Mouse Oocytes. *Cell*. 155(4):807–16

Flemr M, Ma J, Schultz RM, Svoboda P. 2010. P-Body Loss Is Concomitant with Formation of a Messenger RNA Storage Domain in Mouse Oocytes. *Biol Reprod*. 82(5):1008–17

Frank F, Sonenberg N, Nagar B. 2010. Structural basis for 5′-nucleotide base-specific recognition of guide RNA by human AGO2. *Nature*. 465(7299):818–22

Friedman RC, Farh KK-H, Burge CB, Bartel DP. 2009. Most mammalian mRNAs are conserved targets of microRNAs. *Genome Res.* 19(1):92–105

Gantier MP, Williams BRG. 2007. The response of mammalian cells to double-stranded RNA. *Cytokine & Growth Factor Reviews*. 18(5-6):363–71

García-López J, del Mazo J. 2012. Expression dynamics of microRNA biogenesis during preimplantation mouse development. *Biochimica et Biophysica Acta (BBA) - Gene Regulatory Mechanisms*. 1819(8):847–54

García-López J, Hourcade J de D, Alonso L, Cárdenas DB, del Mazo J. 2014. Global characterization and target identification of piRNAs and endo-siRNAs in mouse gametes and zygotes. *Biochimica et Biophysica Acta (BBA) - Gene Regulatory Mechanisms*. 1839(6):463–75

Giraldez AJ, Mishima Y, Rihel J, Grocock RJ, Dongen SV, et al. 2006. Zebrafish MiR-430 Promotes Deadenylation and Clearance of Maternal mRNAs. *Science*. 312(5770):75–79

Girard A, Sachidanandam R, Hannon GJ, Carmell MA. 2006. A germline-specific class of small RNAs binds mammalian Piwi proteins. *Nature*. 442(7099):199–202

Gregory RI, Yan K, Amuthan G, Chendrimada T, Doratotaj B, et al. 2004. The Microprocessor complex mediates the genesis of microRNAs. *Nature*. 432(7014):235–40

Grosswendt S, Filipchyk A, Manzano M, Klironomos F, Schilling M, et al. 2014. Unambiguous Identification of miRNA:Target Site Interactions by Different Types of Ligation Reactions. *Molecular Cell*. 54(6):1042–54

Guo H, Ingolia NT, Weissman JS, Bartel DP. 2010. Mammalian microRNAs predominantly act to decrease target mRNA levels. *Nature*. 466(7308):835–40

Gurtan AM, Sharp PA. 2013. The Role of miRNAs in Regulating Gene Expression Networks. *Journal of Molecular Biology*. 425(19):3582–3600

Han BW, Zamore PD. 2014. piRNAs. *Current Biology*. 24(16):R730–33

Han J. 2004. The Drosha-DGCR8 complex in primary microRNA processing. *Genes & Development*. 18(24):3016–27

Hauptmann J, Dueck A, Harlander S, Pfaff J, Merkl R, Meister G. 2013. Turning catalytically inactive human Argonaute proteins into active slicer enzymes. *Nat Struct Mol Biol*. 20(7):814–17

Hauptmann J, Kater L, Löffler P, Merkl R, Meister G. 2014. Generation of catalytic human Ago4 identifies structural elements important for RNA cleavage. *RNA*. 20(10):1532–38

Helwak A, Kudla G, Dudnakova T, Tollervey D. 2013. Mapping the Human miRNA Interactome by CLASH Reveals Frequent Noncanonical Binding. *Cell*. 153(3):654–65

Huang V, Li L-C. 2014. Demystifying the nuclear function of Argonaute proteins. *RNA Biology*. 11(1):18–24

Jakymiw A, Lian S, Eystathioy T, Li S, Satoh M, et al. 2005. Disruption of GW bodies impairs mammalian RNA interference. *Nature Cell Biology*. 7(12):1267–74

Johnston M, Geoffroy M-C, Sobala A, Hay R, Hutvagner G. 2010. HSP90 Protein Stabilizes Unloaded Argonaute Complexes and Microscopic P-bodies in Human Cells. *Mol. Biol. Cell*. 21(9):1462–69

Kaneda M, Tang F, O'Carroll D, Lao K, Surani MA. 2009. Essential role for Argonaute2 protein in mouse oogenesis. *Epigenetics & Chromatin*. 2(1):9

Kanellopoulou C, Muljo SA, Kung AL, Ganesan S, Drapkin R, et al. 2005. Dicer-deficient mouse embryonic stem cells are defective in differentiation and centromeric silencing. *Genes Dev.* 19(4):489–501

Kelley LA, Sternberg MJE. 2009. Protein structure prediction on the Web: a case study using the Phyre server. *Nature Protocols*. 4(3):363–71

Ketting RF. 2011. The Many Faces of RNAi. *Developmental Cell*. 20(2):148–61

Khvorova A, Reynolds A, Jayasena SD. 2003. Functional siRNAs and miRNAs Exhibit Strand Bias. *Cell*. 115(2):209–16

Kim VN, Jinju Han, Siomi MC. 2009. Biogenesis of small RNAs in animals. *Nature Reviews Molecular Cell Biology*. 10(2):126–39

Knight SW, Bass BL. 2001. A Role for the RNase III Enzyme DCR-1 in RNA Interference and Germ Line Development in Caenorhabditis elegans. *Science*. 293(5538):2269–71

Kozomara A, Griffiths-Jones S. 2014. miRBase: annotating high confidence microRNAs using deep sequencing data. *Nucl. Acids Res.* 42(D1):D68–73

Kuramochi-Miyagawa S, Kimura T, Ijiri TW, Isobe T, Asada N, et al. 2004. Mili, a mammalian member of piwi family gene, is essential for spermatogenesis. *Development*. 131(4):839–49

Kuramochi-Miyagawa S, Watanabe T, Gotoh K, Totoki Y, Toyoda A, et al. 2008. DNA methylation of retrotransposon genes is regulated by Piwi family members MILI and MIWI2 in murine fetal testes. *Genes & Development*. 22(7):908–17

Kwak PB, Tomari Y. 2012. The N domain of Argonaute drives duplex unwinding during RISC assembly. *Nat Struct Mol Biol*. 19(2):145–51

Lee J, Lee D, Park H, Coutsias EA, Seok C. 2010. Protein loop modeling by using fragment assembly and analytical loop closure. *Proteins*. 78(16):3428–36

Lee Y, Ahn C, Han JJ, Choi H, Kim J, et al. 2003. The nuclear RNase III Drosha initiates microRNA processing. *Nature*. 425(6956):415–19

Lee Y, Kim M, Han J, Yeom K-H, Lee S, et al. 2004. MicroRNA genes are transcribed by RNA polymerase II. *The EMBO Journal*. 23(20):4051–60

Leung AKL, Sharp PA. 2013. Quantifying Argonaute Proteins In and Out of GW/P-Bodies: Implications in microRNA Activities. In *Ten Years of Progress in GW/P Body Research*, Vol. 768, eds. EKL Chan, MJ Fritzler, pp. 165–82. New York, NY: Springer New York

Leung AKL, Young AG, Bhutkar A, Zheng GX, Bosson AD, et al. 2011. Genome-wide identification of Ago2 binding sites from mouse embryonic stem cells with and without mature microRNAs. *Nature Structural & Molecular Biology*. 18(2):237–44

Lewis BP, Burge CB, Bartel DP. 2005. Conserved Seed Pairing, Often Flanked by Adenosines, Indicates that Thousands of Human Genes are MicroRNA Targets. *Cell*. 120(1):15–20

Lewis BP, Shih I -hun., Jones-Rhoades MW, Bartel DP, Burge CB. 2003. Prediction of Mammalian MicroRNA Targets. *Cell*. 115(7):787–98

Li L, Lu X, Dean J. 2013a. The maternal to zygotic transition in mammals. *Molecular Aspects of Medicine*. 34(5):919–38

Lin H, Spradling AC. 1997. A novel group of pumilio mutations affects the asymmetric division of germline stem cells in the Drosophila ovary. *Development*. 124(12):2463–76

Liu J, Carmell MA, Rivas FV, Marsden CG, Thomson JM, et al. 2004. Argonaute2 Is the Catalytic Engine of Mammalian RNAi. *Science*. 305(5689):1437–41

Liu J, Rivas FV, Wohlschlegel J, Yates JR, Parker R, Hannon GJ. 2005a. A role for the P-body component GW182 in microRNA function. *Nature Cell Biology*. 7(12):1261–66

Liu J, Valencia-Sanchez MA, Hannon GJ, Parker R. 2005b. MicroRNA-dependent localization of targeted mRNAs to mammalian P-bodies. *Nature Cell Biology*. 7(7):719–23

Li Y, Lu J, Han Y, Fan X, Ding S-W. 2013b. RNA Interference Functions as an Antiviral Immunity Mechanism in Mammals. *Science*. 342(6155):231–34

Lund E, Liu M, Hartley RS, Sheets MD, Dahlberg JE. 2009. Deadenylation of maternal mRNAs mediated by miR-427 in Xenopus laevis embryos. *RNA*. 15(12):2351–63

Lykke-Andersen K, Gilchrist MJ, Grabarek JB, Das P, Miska E, Zernicka-Goetz M. 2008. Maternal Argonaute 2 Is Essential for Early Mouse Development at the Maternal-Zygotic Transition. *Mol. Biol. Cell*. 19(10):4383–92

Maillard PV, Ciaudo C, Marchais A, Li Y, Jay F, et al. 2013. Antiviral RNA Interference in Mammalian Cells. *Science*. 342(6155):235–38

Ma J, Flemr M, Stein P, Berninger P, Malik R, et al. 2010. MicroRNA Activity Is Suppressed in Mouse Oocytes. *Current Biology*. 20(3):265–70

Ma J, Flemr M, Strnad H, Svoboda P, Schultz RM. 2013. Maternally Recruited DCP1A and DCP2 Contribute to Messenger RNA Degradation During Oocyte Maturation and Genome Activation in Mouse. *Biol Reprod*. 88(1):11

Mathys H, Basquin J, Ozgur S, Czarnocki-Cieciura M, Bonneau F, et al. 2014. Structural and Biochemical Insights to the Role of the CCR4-NOT Complex and DDX6 ATPase in MicroRNA Repression. *Molecular Cell*. 54(5):751–65

Meister G. 2013. Argonaute proteins: functional insights and emerging roles. *Nature Reviews Genetics*. 14(7):447–59

Meister G, Landthaler M, Patkaniowska A, Dorsett Y, Teng G, Tuschl T. 2004. Human Argonaute2 mediates RNA cleavage targeted by miRNAs and siRNAs. *Mol. Cell*. 15(2):185–97

Murchison EP, Partridge JF, Tam OH, Cheloufi S, Hannon GJ. 2005. Characterization of Dicer-deficient murine embryonic stem cells. *PNAS*. 102(34):12135–40

Murchison EP, Stein P, Xuan Z, Pan H, Zhang MQ, et al. 2007. Critical roles for Dicer in the female germline. *Genes Dev.* 21(6):682–93

Nakanishi K, Ascano M, Gogakos T, Ishibe-Murakami S, Serganov AA, et al. 2013. Eukaryote-Specific Insertion Elements Control Human ARGONAUTE Slicer Activity. *Cell Reports*. 3(6):1893–1900

Nejepinska J, Malik R, Wagner S, Svoboda P. 2014. Reporters Transiently Transfected into Mammalian Cells Are Highly Sensitive to Translational Repression Induced by dsRNA Expression. *PLoS ONE*. 9(1):e87517

Pal-Bhadra M, Bhadra U, Birchler JA. 2002. RNAi related mechanisms affect both transcriptional and posttranscriptional transgene silencing in Drosophila. *Mol. Cell*. 9(2):315–27

Park S-J, Komata M, Inoue F, Yamada K, Nakai K, et al. 2013. Inferring the choreography of parental genomes during fertilization from ultralarge-scale whole-transcriptome analysis. *Genes Dev.* 27(24):2736–48

Pauli A, Rinn JL, Schier AF. 2011. Non-coding RNAs as regulators of embryogenesis. *Nature Reviews Genetics*. 12(2):136–49

Pfaff J, Hennig J, Herzog F, Aebersold R, Sattler M, et al. 2013. Structural features of Argonaute–GW182 protein interactions. *PNAS*. 110(40):E3770–79

Pfeiffer MJ, Taher L, Drexler H, Suzuki Y, Makałowski W, et al. 2015. Differences in embryo quality are associated with differences in oocyte composition: A proteomic study in inbred mice. *PROTEOMICS*. 15(4):675–87

Pillai RS, Bhattacharyya SN, Artus CG, Zoller T, Cougot N, et al. 2005. Inhibition of Translational Initiation by Let-7 MicroRNA in Human Cells. *Science*. 309(5740):1573–76

Reuter M, Berninger P, Chuma S, Shah H, Hosokawa M, et al. 2011. Miwi catalysis is required for piRNA amplification-independent LINE1 transposon silencing. *Nature*. 480(7376):264–U154

Reynolds A, Anderson EM, Vermeulen A, Fedorov Y, Robinson K, et al. 2006. Induction of the interferon response by siRNA is cell type– and duplex length–dependent. *RNA*. 12(6):988–93

Rivas FV, Tolia NH, Song J-J, Aragon JP, Liu J, et al. 2005. Purified Argonaute2 and an siRNA form recombinant human RISC. *Nature Structural & Molecular Biology*. 12(4):340–49

Sagan SM, Sarnow P. 2013. RNAi, Antiviral After All. *Science*. 342(6155):207–8

Schirle NT, MacRae IJ. 2012. The Crystal Structure of Human Argonaute2. *Science*. 336(6084):1037–40

Schirle NT, Sheu-Gruttadauria J, MacRae IJ. 2014. Structural basis for microRNA targeting. *Science*. 346(6209):608–13

Schürmann N, Trabuco LG, Bender C, Russell RB, Grimm D. 2013. Molecular dissection of human Argonaute proteins by DNA shuffling. *Nat Struct Mol Biol*. 20(7):818–26

Schwarz DS, Hutvágner G, Du T, Xu Z, Aronin N, Zamore PD. 2003. Asymmetry in the Assembly of the RNAi Enzyme Complex. *Cell*. 115(2):199–208

Schwarz DS, Tomari Y, Zamore PD. 2004. The RNA-Induced Silencing Complex Is a Mg2+-Dependent Endonuclease. *Current Biology*. 14(9):787–91

Selbach M, Schwanhäusser B, Thierfelder N, Fang Z, Khanin R, Rajewsky N. 2008. Widespread changes in protein synthesis induced by microRNAs. *Nature*. 455(7209):58–63

Sen GL, Blau HM. 2005. Argonaute 2/RISC resides in sites of mammalian mRNA decay known as cytoplasmic bodies. *Nature Cell Biology*. 7(6):633–36

Shenoy A, Blelloch RH. 2014. Regulation of microRNA function in somatic stem cell proliferation and differentiation. *Nature Reviews Molecular Cell Biology*. 15(9):565–76

Siomi MC, Sato K, Pezic D, Aravin AA. 2011. PIWI-interacting small RNAs: the vanguard of genome defence. *Nature Reviews Molecular Cell Biology*. 12(4):246–58

Sonenberg N, Hinnebusch AG. 2009. Regulation of Translation Initiation in Eukaryotes: Mechanisms and Biological Targets. *Cell*. 136(4):731–45

Stein P, Rozhkov NV, Li F, Cárdenas FL, Davydenk O, et al. 2015. Essential Role for Endogenous siRNAs during Meiosis in Mouse Oocytes. *PLOS Genetics*. 11(2):e1005013

Stein P, Svoboda P, Anger M, Schultz RM. 2003. RNAi: Mammalian oocytes do it without RNA-dependent RNA polymerase. *RNA*. 9(2):187–92

Stry MV, Oguin TH, Cheloufi S, Vogel P, Watanabe M, et al. 2012. Enhanced Susceptibility of Ago1/3 Double-Null Mice to Influenza A Virus Infection. *J. Virol.* 86(8):4151–57

Suh N, Baehner L, Moltzahn F, Melton C, Shenoy A, et al. 2010. MicroRNA Function Is Globally Suppressed in Mouse Oocytes and Early Embryos. *Current Biology*. 20(3):271–77

Svoboda P. 2014. Renaissance of mammalian endogenous RNAi. *FEBS Letters*. 588(15):2550–56

Svoboda P, Flemr M. 2010. The role of miRNAs and endogenous siRNAs in maternal-to-zygotic reprogramming and the establishment of pluripotency. *EMBO reports*. 11(8):590–97

Svoboda P, Stein P, Hayashi H, Schultz RM. 2000. Selective reduction of dormant maternal mRNAs in mouse oocytes by RNA interference. *Development*. 127(19):4147–56

Swarts DC, Makarova K, Wang Y, Nakanishi K, Ketting RF, et al. 2014. The evolutionary journey of Argonaute proteins. *Nature Structural & Molecular Biology*. 21(9):743–53

Tam OH, Aravin AA, Stein P, Girard A, Murchison EP, et al. 2008. Pseudogene-derived small interfering RNAs regulate gene expression in mouse oocytes. *Nature*. 453(7194):534–38

Tang F, Kaneda M, O'Carroll D, Hajkova P, Barton SC, et al. 2007. Maternal microRNAs are essential for mouse zygotic development. *Genes Dev.* 21(6):644–48

Tanguy M, Miska EA. 2013. Antiviral RNA interference in animals: piecing together the evidence. *Nature Structural & Molecular Biology*. 20(11):1239–41

Walser CB, Lipshitz HD. 2011. Transcript clearance during the maternal-to-zygotic transition. *Current Opinion in Genetics & Development*. 21(4):431–43

Wang Q, Carmichael GG. 2004. Effects of Length and Location on the Cellular Response to Double-Stranded RNA. *Microbiol Mol Biol Rev*. 68(3):432–52

Wang S, Kou Z, Jing Z, Zhang Y, Guo X, et al. 2010. Proteome of mouse oocytes at different developmental stages. *PNAS*. 107(41):17639–44

Wang Y, Juranek S, Li H, Sheng G, Wardle GS, et al. 2009. Nucleation, propagation and cleavage of target RNAs in Ago silencing complexes. *Nature*. 461(7265):754–61

Watanabe T, Takeda A, Tsukiyama T, Mise K, Okuno T, et al. 2006. Identification and characterization of two novel classes of small RNAs in the mouse germline: retrotransposon-derived siRNAs in oocytes and germline small RNAs in testes. *Genes Dev.* 20(13):1732–43

Watanabe T, Totoki Y, Toyoda A, Kaneda M, Kuramochi-Miyagawa S, et al. 2008. Endogenous siRNAs from naturally formed dsRNAs regulate transcripts in mouse oocytes. *Nature*. 453(7194):539–43

Wee LM, Flores-Jasso CF, Salomon WE, Zamore PD. 2012. Argonaute Divides Its RNA Guide into Domains with Distinct Functions and RNA-Binding Properties. *Cell*. 151(5):1055–67

Weick E-M, Miska EA. 2014. piRNAs: from biogenesis to function. *Development*. 141(18):3458–71

Wianny F, Zernicka-Goetz M. 2000. Specific interference with gene function by double-stranded RNA in early mouse development. *Nat Cell Biol*. 2(2):70–75

Wilson RC, Doudna JA. 2013. Molecular Mechanisms of RNA Interference. *Annu. Rev. Biophys.* 42(1):217–39

Yeom K-H, Lee Y, Han J, Suh MR, Kim VN. 2006. Characterization of DGCR8/Pasha, the essential cofactor for Drosha in primary miRNA processing. *Nucleic Acids Research*. 34(16):4622–29

Yi R, Qin Y, Macara IG, Cullen BR. 2003. Exportin-5 mediates the nuclear export of pre-microRNAs and short hairpin RNAs. *Genes Dev.* 17(24):3011–16

Zekri L, Kuzuoğlu-Öztürk D, Izaurralde E. 2013. GW182 proteins cause PABP dissociation from silenced miRNA targets in the absence of deadenylation. *The EMBO Journal*. 32(7):1052–65